PRECONCENTRATION OF CYSTEINE IN A MICROFLUID DEVICE USING GMA-EDMA MONOLITH

MISS NISARAT PROMTRAKULCHAI

A SPECIAL RESEARCH PROJECT SUBMITTED IN PARTIAL FULFILLMENT
OF THE REQUIREMENTS FOR
THE DEGREE OF MASTER OF ENGINEERING (CHEMICAL ENGINEERING)
FACULTY OF ENGINEERING
KING MONGKUT'S UNIVERSITY OF TECHNOLOGY THONBURI
2011

Preconcentration of cysteine in a microfluid device using GMA-EDMA monolith

Miss Nisarat Promtrakulchai B.Eng. (Chemical Engineering)

A Special Research Project Submitted in Partial Fulfillment
of the Requirements for
the Degree of Master of Engineering (Chemical Engineering)
Faculty of Engineering
King Mongkut's University of Technology Thonburi
2011

Special Research Project Committee

..... Chairman
(Asst. Prof. Asawin Meechai, Ph.D.)

..... Member and Special
(Asst. Prof. Kwanchanok Pasuwat, Ph.D.) Research Project Advisor

..... Member
(Dr. Nonsee Nimitsiriwat, Ph.D.)

Special Research Project Title	Preconcentration of Cysteine in a microfluid device using GMA-EDMA Monolith
Special Research Project Credits	6
Candidate	Miss Nisarat Promtrakulchai
Special Research Project Advisor	Asst. Prof. Dr. Kwanchanok Pasuwat
Program	Master of Engineering
Field of Study	Chemical Engineering
Department	Chemical Engineering
Faculty	Engineering
B.E.	2554

Abstract

Nowadays, physical and biological sciences have been developed continuously. Many new technologies have been applied to analyze various diseases. Lab-on-a-chip devices are used widely in biomedical and other analytical applications including rapid pathogen detection, clinical diagnosis, forensic science, and electrophoresis. The analytical components in the device are connected via small fluid volume channels in micro or nano liters, called microfluidics. It can measure very small volume of sample within a short amount of time. Several materials can be used for the fabrication of microfluidic devices including glass and polymer or combinations of these materials. Although microfluidic devices have great potential, there are limitations that the concentration of analyte in a sample is often near the detection limit, leading to unreliable performance. Therefore, preconcentration of a sample in microfluidic devices is necessary. There has been an interest in developing a sample preconcentration system by increasing the concentration of a sample via chemical adsorption on the surface. To increase the concentration in the sample, the monolithic polymer was synthesized in a glass capillary by UV-polymerazation using GMA and EDMA as monomers in a porogenic solvent which consists of methanol and ethanol and DAP as an initiator. The epoxide groups on the monolith surface were transformed to 3-mercapoto-2-hydroxy-propyl in a nucleophilic substitution reaction using sodium-hydrogen sulfide (NaSH) as a necleophilic reagent. Thus, modified-monolith can be used as a solid phase to adsorb the sample solution in the second step. The monoliths prepared from various monomer concentrations (12.5, 25, and 50 percent by weight) at different polymerization times (10, 20, and 30 min) were characterized using Scanning Electron Microscope (SEM) and BET for structural analysis. The results show that the monolith using a higher monomer concentration and longer polymerization time possessed higher surface area with smaller micropore and bead size. The amount of reactive thiol groups generated on the monolith surface could be determined from a disulfide-exchanger reaction using 2,2’ dipyridyl disulfide. About 16% of total epoxide moieties of the monolithic substrate could be transformed to reactive sulfhydryl groups on the 50% monomer concentration polymerized for 30 min. Cysteine, an essential amino acid in human body commonly used to investigate several diseases, was selected as a model of thiol compound for our study. Cysteine in aqueous solution was injected into the system at 10 µl/min and formed a disulfide bond with the thiol group on the surface of the monolith. The inlet cysteine concentration at 0.3 millimolar gave the maximum adsorption efficiency. Cysteine adsorbed on the monolith was then eluted using TCEP at 50 molar in excess. The maximum fold increase was 18.45 when the elution rate was at 3µl/hr.

Keyword: amino acid/ microfluid/ monolithic polymer/ preconcentration / thiol groups

หัวข้อโครงการศึกษาวิจัย	การศึกษาระบบเพิ่มความเข้มข้นของสารตัวอย่างซิสเทอีนในเครื่องไมโครฟลูอิดิกโดยใช้โมโนลิทชนิด GMA-EDMA
หน่วยกิต	6
ผู้เขียน	นางสาวนิศารัตน์ พร้อมตระกูลชัย
อาจารย์ที่ปรึกษา	ผศ.ดร.ขวัญชนก พสุวัต
หลักสูตร	วิศวกรรมศาสตรมหาบัณฑิต
สาขาวิชา	วิศวกรรมเคมี
ภาควิชา	วิศวกรรมเคมี
คณะ	วิศวกรรมศาสตร์
พ.ศ.	2554

บทคัดย่อ

ในปัจจุบัน วิทยาศาสตร์ทางกายภาพและชีวภาพได้มีการพัฒนาขึ้นอย่างต่อเนื่อง มีเทคโนโลยีใหม่จำนวนมากได้ถูกนำมาใช้ในการวิเคราะห์โรคต่างๆ การพัฒนาของแล็บบนชิพได้รับความสนใจมากในปีที่ผ่านมา แล็บบนชิพใช้กันอย่างแพร่หลายในการวิเคราะห์ทางการแพทย์และอื่นๆ รวมถึงการตรวจจับเชื้อโรคอย่างรวดเร็ว, การวินิจฉัยทางคลินิกนิติวิทยาศาสตร์ และอิเล็กโตรโฟรีซิท ประเภทของอุปกรณ์ชนิดนี้จะเชื่อมต่อผ่านช่องผ่านสารขนาดเล็กในระดับไมโครหรือนาโนลิตร ที่เรียกว่า ไมโครฟลูอิดิก เครื่องมือนี้ถูกใช้สำหรับการแยกสารทางชีวภาพขนาดย่อ และช่วยในการวิเคราะห์สารหลายๆรายการโดยดำเนินการแบบคู่ขนานไปกับอุปกรณ์ขนาดเล็ก จุดเด่นของเครื่องมือชนิดนี้คือสามารถวิเคราะห์สารตัวอย่างที่มีปริมาณน้อยมากได้ในระยะเวลาอันสั้น ไมโครฟลูอิดิกถูกสร้างขึ้นโดยใช้วัสดุประเภทแก้ว, โพลีเมอร์สังเคราะห์ หรือ การรวมกันของวัสดุเหล่านี้ โพลีไดเมทิลไซลอกเซนหรือพีดีเอ็มเอสเป็นสารโพลิเมอร์ที่ส่วนใหญ่นำมาใช้ในการขึ้นรูปเครื่องไมโครฟลูอิดิกส์เนื่องจากหาง่ายและราคาถูก แต่ในงานวิจัยนี้จะใช้หลอดแก้วคะปิลารีเป็นช่องผ่านของสารเสมือนเป็นไม่โครฟลูอิดิก ถึงแม้ว่าอุปกรณ์ชนิดนี้จะมีศักยภาพที่ดี แต่ยังคงมีข้อจำกัดที่ควรได้รับการพัฒนา คือ ปริมาณสารตัวอย่างที่ใช้ในวิเคราะห์มีปริมาณน้อยมาก นำไปสู่ความคลาดเลื่อน ระบบเพิ่มความเข้มข้นจึงถูกนำมาใช้เพื่อแก้ปัญหาดังกล่าว ดังนั้นในงานวิจัยนี้ จึงมีความสนใจในการพัฒนาระบบเพิ่มความเข้มข้นของสารตัวอย่าง โดยอาศัยกระบวนการดูดซับทางเคมีบนพื้นผิว สำหรับการเพิ่มความเข้มข้นของสารตัวอย่าง โมโนลิติกโพลิเมอร์จะถูกสังเคราะห์ขึ้นภายในหลอดแก้วคะปิลารี่ โดยใช้แสงยูวีเพื่อใช้เป็นตัวดูดซับสารที่ต้องการเพิ่มความเข้มข้น และใช้ไกลซิดิลเมทาคริเลตและเอธิลีนไดเมธาคริเลตเป็นสารโมโนเมอร์ ซึ่งตัวทำละลาย ได้แก่ เมทานอลและ เอทานอล กลุ่มอิพ๊อกไซด์บนโมโนลิติกโพลีเมอร์จะถูกเปลี่ยนไปเป็นกลุ่มไธออล หลังจากทำปฏิกิริยากับโซเดียมไอโดรเจนซัลไฟล์ ตัวแปรที่ถูกสนใจว่าส่งผลต่อโครงสร้างของโมโนลิติกโพลิเมอร์ ได้แก่ ความเข้มข้นของโมโน

เมอร์และระยะเวลาในการสังเคราะห์โพลิเมอร์ ดังนั้นเพื่อหาสภาวะที่ดีที่สุด จึงได้ศึกษาโครงสร้างของโมโนลิติกโพลิเมอร์ที่ถูกสังเคราะห์ ณ สภาวะต่างๆ ได้แก่ การโพลิเมอร์ไรเซชั่นที่ความเข้มข้นของมอนอเมอร์เป็นร้อยละ 12.5, 25, และ50 โดยน้ำหนัก และระยะเวลาในการโพลิเมอร์ไรเซชั่นเป็น 10, 20, และ 30 นาที โดยใช้กล้องจุลทรรศน์อิเล็กตรอนแบบส่องกราดและเครื่องวัดพื้นที่ผิวเป็นเครื่องมือวิเคราะห์โครงสร้าง จากการทดลองพบว่า เมื่อความเข้มข้นของโมโนเมอร์และระยะเวลาในการโพลิเมอร์ไรเซชั่นเพิ่มขึ้น ส่งผลให้พื้นที่ผิวของโพลิเมอร์เพิ่มขึ้น ในขณะที่ ขนาดของเม็ดบีดโพลิเมอร์ รูพรุนขนาดกลางลดลง ดังนั้นเพื่อโครงสร้างที่เหมาะสมแก่การเพิ่มความเข้มข้นของสาร โมโนลิติกโพลิเมอร์ควรสังเคราะห์จากโมโนเมอร์ที่มีความเข้มข้นร้อยละ 50 โดยน้ำหนัก และใช้ระยะเวลาสังเคราะห์ทั้งสิ้น 30 นาที ซึ่งเป็นสภาวะที่ทำให้เกิดพื้นที่ผิวสัมผัสในการถ่ายเทมวลสารมาก การหาปริมาณของกลุ่มไธออลที่เกิดขึ้นพิจารณาจากการทำปฏิกริยาแลกเปลี่ยนพันธะไดซัลไฟล์ ด้วย DPDS จากการทดลองพบว่า ประมาณ 17% ของกลุ่มอิพ๊อกไซด์ ถูกเปลี่ยนไปเป็นกลุ่มไธออล บนโมโนลิติกโพลีเมอร์ที่มีความเข้มข้นร้อยละ 50 โดยน้ำหนัก และใช้ระยะเวลาสังเคราะห์ทั้งสิ้น 30 นาที สำหรับสารตัวอย่างที่ต้องการเพิ่มความเข้มข้น คือ ซิสเทอีน ซึ่งเป็นกรดอะมิโนชนิดหนึ่งที่สามารถใช้เป็นตัวบ่งชี้ในการวิเคราะห์โรคต่างๆได้ ผลจากการศึกษาพบว่า ประสิทธิภาพในการดูดซับจะดีที่สุดเมื่อฉีดซิสเทอีนที่อัตราการไหลโดยปริมาตรเท่ากับ 10 ไมโครลิตรต่อนาที และความเข้มข้นของซิสเทอีนเท่ากับ 0.3 มิลลิโมลาร์ จากนั้นซิสเทอีนที่ถูกดูดซับในโมโนลิติกโพลิเมอร์จะถูกสกัดออกมาโดยใช้ TCEPที่มีความเข้มข้นมากกว่า 50 เท่าของปริมาณซิสเทอีนที่ถูกดูดซับ โดยความเข้มข้นของซิสเทอีนหลังการเพิ่มความเข้มข้นสามารถเพิ่มขึ้นได้เป็น18.45 เท่าของความเข้มข้นเดิม

คำสำคัญ : กรดอะมิโน/ กลุ่มไธออล/ การเพิ่มความเข้มข้น/ โมโนลิติกพอลิเมอร์/ ไมโครฟลูอิดิก

ACKNOWLEDGEMENTS

First and foremost, the author would like to express the gratitude to my advisor, Asst.Prof.Dr. Kwanchanok Pasuwat for her excellent guidance and encouragement. The author also thanked to Asst. Prof. Asawin Meechai and Dr.Nonsee Nimitsiriwat, members of committee, for valuable discussion and assistance. They provided new insights and elucidations to several theoretical and practical problems during this study. It was gratefully acknowledged to all staffs at Chemical Engineering Laboratory at KMUTT for the facilities in experiment rooms, equipments, and BET analysis, and the food engineering department for their help in syringe pump.

Furthermore, I would like to extend my appreciation to Chemical Engineering Practice School (ChEPS) teachers for their valuable vision. Lastly, I would like to thank my family members and all pals for their dedicated support.

CONTENTS

LIST OF TABLES

LIST OF FIGURES

CHAPTER 1 INTRODUCTION

1.1Background

Nowadays, physical and biological sciences have been developed continuously. Many new technologies have been applied to analyze various diseases. The development of lab-on-a-chip devices has received much attention in the recent years. The lab-on-chip devices are used widely in biomedical and other analytical applications including rapid pathogen detection, clinical diagnosis, forensic science, and electrophoresis [1]. This type of device integrates interesting functions on a single chip and scales down a laboratory from millimeters to a few square centimeters in size. The chip connected via small fluid volume channels in micro or nano liters, called microfluidics.

Microfluidics is the miniaturization of biological separation and assay techniques, allowing multiple experiments to be performed in parallel on a small device. In this technology, minute quantities of fluid and even nanoparticles are flown- through the tiny channels using flow control device (e.g. channels pumps, mixers and valves). It can measure very small volume of sample within a short amount of time. The microfluidic technology has an ability to detect extremely low concentration of small molecules, protein, toxins and microganisms to analyze several diseases in human bodies.

Several materials can be used for the fabrication of microfluidic devices including glass and polymer or combinations of these materials [2]. Most of early devices were fabricated from silicon since the techniques for the fabrication using this material was well-developed. It was later found that silicon was too expensive and had further disadvantage that it is opaque in the visible/UV light. Therefore, silicon is not an appropriate material for the systems that use light detection. The material of choice was then shifted to polymer. The fabrication of polymer devices is easy and reduces the cost of manufacturing. The microchannels can be molded by soft lithography. Polydimethylsiloxane (PDMS) is the most actively developed polymer for the fabrication of microfluidics. PDMS is optically clear and general considered being inert, non-toxic and non-flammable.

Although microfluidic devices have great potential, there are several challenges that need to be overcome. One of the frequently encountered limitations is that the concentration of analyte in a sample is often near the detection limit, leading to unreliable performance. Therefore, preconcentration of a sample in microfluidic devices is necessary. There has been an interest in developing an on-chip sample preconcentration to improve the efficiency of the microfluidic chips by increasing the concentration of a sample via surface adsorption. The previously successful sample preconcentration system used solid phase adsorption by using monolithic polymer as solid phase. The monolith can be synthesized by the UV polymerization using a mixture of monomer in a porogenic solvent and an initiator. The monolithic polymer is prepared in the microchannel where fluid flows through. As the sample flows through the small channel, the analyte is adsorped onto the surface of the porous monolith while the remaining sample flows out. After that, stronger solvent is added to the channel to elute the sample trapped in the pore. Low volume of solvent was used to elute the analyte, leading to an increase in the concentration of the test sample.

In the previous research on "Development of a microfluidic sample preconcentration system for cysteine using BuMA-EDMA monolithic" by Supakarnpitayakul, butyl methacrylates (BuMA) and ethylene dimethacrylate (EDMA) was selected as the monolithic polymer in 1-deconol and cyclohexanol as porogenic mixture. The major factor that affected the adsorption efficiency was the surface area of the monolith. This system was able to increase the concentration of samples containing cysteine to about 8.17 fold. However, the concentration of cytsteine was not high enough for reliable performance. It was concluded that physical adsorption alone was not sufficient. Chemical adsorption was then suggested. Therefore, the aim of this project is to modify the surface of the monolith to allow for chemisorption of cysteine. Glycidyl methacrylate (GMA) and ethylene dimethacrylate (EDMA) were selected as monolith polymers because of their ability to generate the reactive thiol group on the surface. The epoxide groups of poly (GMA-co-EDMA) are transformed to 3-mercapoto-2-hydroxy-propyl in a nucleophilic substitution reaction by using sodium-hydrogen sulfide (NaSH) as a necleophilic reagent. Thus the modified-monolith can be utilized to attach a chromatographic ligand in the second step by versatile chemistries, e.g. by radical addition, graft polymerization, nucleophilic substitution, disulfide formation and Michael addition reaction [3].

In this project, cysteine was selected as a model of a thiol compound. Cysteine is one of important amino acids that can be used in an early detection of various diseases. In plasma, total cysteine is found at the highest concentration reaching 250 mM [50]. Its main function is to remove toxin from the liver and protects the liver and the brain. The previous reports have shown that cysteine can be used as a biomarker for the detection of prostate cancer [4]. Altered levels of cysteine have been implicated in hyperhomocysteinemiathis and in a number of pathological conditions including Alzheimer's and Parkinson'sdisease [50]. Thus, the accurate measurement is essential. Cysteine has a sulfur atom which involves in the formation of thiol group. It is believed that cysteine is able to form a disulfide bridge with the modified-monolith. Since the formation of a disulfide bond is preferred over the Van de Waal force in physical adsorption, the adsorption efficiency will be increased, leading to an increase in the concentration of cysteine in the sample after elution.

1.2 Objectives

1. To modify the surface of monolithic polymer by generating thiol groups and characterize the surface of the monolith.

2. To study the effect of the monomer concentration and polymerization time on the monolith's morphology.

3. To determine the adsorption and elution efficiencies of the preconcentration system.

4. To evaluate whether this system can be used as an on-chip sample preconcentration based on number of fold-increase in the concentration of cysteine.

1.3 Scope of work

1. The GMA-EDMA was selected as a monolithic monomer.

2. The nucleophilic reagent was sodium-hydrogen sulfide (NaSH) which was used to generate a thiol group.

3. The tris(2-carboxyethyl) phosphine hydrochloride (TCEP) was used as a reduction reagent to remove disulfide bond on the monolith's surface.

1.4 Expected results

An on-chip preconcentration system will be fabricated using the polymerized monolithic polymer which is surface-modified to allow for the chemical adsorption of the test compound. The concentration of cysteine in the test sample is expected to be increased at least 10 fold.

CHAPTER 2 LITERATURE REVIEW

2.1 Microfluidic Device

The microfluidic devices emerged in the beginning of the 1980s and have been rapidly developed with application in the medical, pharmaceutical and chemical industries [5]. The microfluidic chip is the device which manipulates the fluids in a small channel with dimension of micrometers. The advantage is association with analytical miniaturization. The initially fabricated in silicon and glass using photolithography and etching techniques adapted from the microelectronics industry, which are precise but expensive and flexible [6]. Therefore, the material was then shifted to polymer. Poly (dimethylsiloxane) (PDMS) is one of the most utilized polymeric materials to fabricate microfluidic devices.

2.1.1 PDMS

The elastomeric material is PDMS have emerged recently as excellent alternatives to the silicon and glass used in early devices fabricated by microelectromechanical systems processes. The chemical formula of PDMS is $CH_3[Si(CH_3)_2O]_nSi(CH_3)_3$ where n is the number of repeating monomer $[SiO(CH_3)_2]$ units [7]. The structure of PDMS is shown as following.

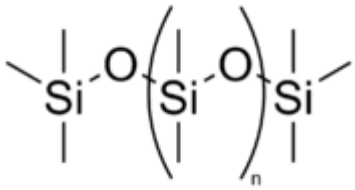

Figure 2.1 Chemical structure of PDMS [7].

The PDMS has essential characteristics that it is elastomeric, can be optically transparent, chemically inert, permeable to gases and amenable to fabrication via rapid prototyping. The PDMS has several dominant characteristics for instances a low glass transition temperature ($Tg \approx -125\ ^{\circ}C$), a unique flexural strength (the shear modulus G may vary between 100 kPa and 3 MPa), high dielectric strength ($\sim$21 kV mm$-$1), high gas permeability, high compressibility, usability over a wide temperature range (at least from -50 °C up to +200 °C), low chemical reactivity (except at high pH levels), a non-toxicity, and its transparency down to 300 nm and resulting in the curing by UV- cross linking of a molded prepolymer [8]. After polymerization and cross-linking, solid PDMS samples will present an external hydrophobic surface. This surface makes it difficult for polar solvents (such as water) to wet the PDMS surface, and may leads to adsorption of hydrophobic contaminants. Plasma oxidation can be used to alter the surface chemistry by adding silanol (SiOH) groups to the surface. This treatment provides the PDMS surface hydrophilic, allowing water to wet. The oxidized surface resists adsorption of hydrophobic and negatively charged species [7].

The PDMS is commonly used as a stamp resin in the procedure of soft lithography. It is the most common material is used for flow delivery in the microfluidic device. It can reach to 6 nm in size [9]. In Bio-MEMS, soft lithography technique is used for fabrication of microfluidic device in both organic and inorganic contexts. The silicon wafers are used to design channels, and the PDMS is then poured over these wafers and

left to harden. Then removed it, This PDMS block is modified the surface by using RF Plasma technique. Once surface bonds are disrupted, usually a piece of glass slide is placed on the activated side of the PDMS (the side with imprints). The glass is permanently sealed to the PDMS to create a waterproof channel. Researchers can utilize various different surface chemistry techniques with these devices for different functions creating unique lab-on-a-chip devices for rapid parallel testing [10].

2.1.2 The Soft Lithography

The soft lithography technique is a fabrication method base on printing and molding organic material. The Soft lithography is generally used to construct features measured on the micrometer to nanometer scale. According to Rogers and Nuzzo (2005), the development of soft lithography expanded rapidly during the period 1995 to 2005 [11] for application in microcontact printing (μCP), microtransfer molding (μTM), and molding in capillaries (MIMIC). The Soft lithography has some advantage over other form of lithography. Comparing with photolithography, it is lower cost than traditional photolithography in mass production and more pattern-transferring methods than traditional lithography techniques. Moreover, it has small detail in laboratory setting (30 nm to 6nm).

For fabrication, starting with fabrication of master by using SU-8 photoresist spins coating on silicon or aluminium wafer. The SU-8 photoresist is a very viscous polymer that can be spun or spread over a thickness from 0.1 micrometer up to 2 millimeters and still be processed with a standard mask aligner. The first layer of SU-8 exposes to UV light to form crosslink on surface. The SU-8 spans on the surface for second time. The second layer is created on the first layer. The thickness of the second layer is equal to the required depth of the microfluidic channel. The second layer is performed in a UV mask aligner at a wavelength of 365 nm. After bake, the exposed photoresist is finally developed to dissolve the unexposed SU-8 and a SU-8 pattern already to be used as a mold for PDMS. The PDMS channel is generated using soft lithography technique. The PDMS mixer is poured onto the SU-8 wafer and cured at 120 °C for 30 min to form crosslink. After curing, the PDMS layer is peeled off from the SU-8 wafer. Then, two holes of channel are punched through the PDMS layer [12-14]. The step of soft lithography to fabricate PDMS can be briefly shown as following figure.

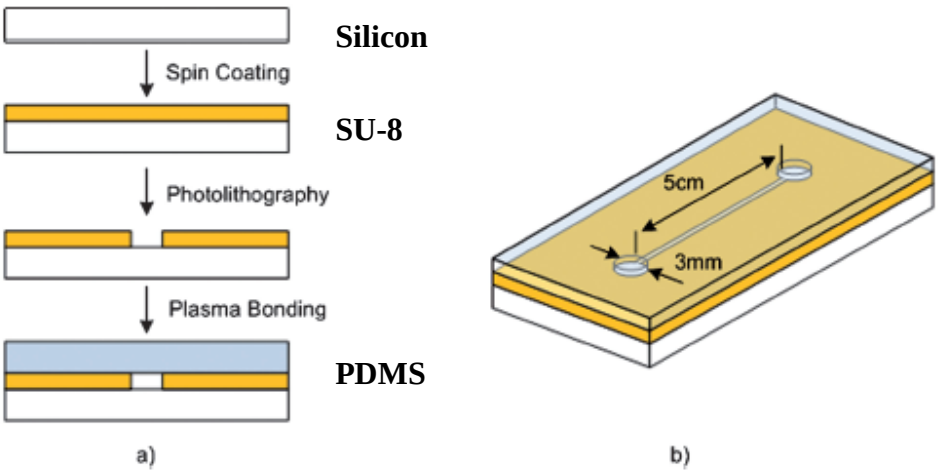

Figure 2.2 (a)The step of soft lithography to fabricate PDMS master (b) side view of microchip [14].

2.2 Monolithic Polymerization

Porous monolithic polymers are a new category of materials developed during last ten years. The porous polymer is called “monolith” is used as a pack column inside a microfluidic channel. Polymerization of a mixture that typically contains monomers, free-radical initiator, and porogenic solvent afford macroporous materials with large pores that enable fluids flow. The advantage of the monolithic polymer compared with other materials is its high permeability to flow liquid at low to moderate back pressure due to the presence of interconnection of macropore and mesopore.

The applications of monolithic materials are demonstrated on the chromatographic separation of biological compounds and synthetic polymers, electrochromatography, gas chromatography, enzyme immobilization, molecular recognition, and in advanced detection systems. Grafting of the pore walls with selected polymers leads to materials with completely changed surface chemistries [21].

Figure 2.3 The channel with monolithic.

Furthering research, Svec and Frechet developed monolithic materials in a column format.These monolith is prepared by in situ polymerization into the chromatographic tube. On the other hand, the use of sol-gel chemistry to develop porous silica monoliths was introduced by Tanaka and Siouffi. Then, the processes developed to improve the characteristics and performance of monolithic materials has developed into versatile and efficient alternatives to polymeric beads for a wide range of applications. Nowadays, monoliths can be formed in situ into any geometry (disks, rods and capillary columns) and advantageously made in sizes ranging from several liters to a few nanoliters in the channel of a microfluidic chip [22].

Initially, the porous monolithic polymer has been prepared by thermal initiated polymerization. However, this method was not suitable enough to prepare in the microfluidic device because it is difficult to specify the heating area on the desired space precisely. UV initiated polymerization (or photoinitiated polymerization) was developed as another method. The UV polymerization has great advantages in much faster preparation than the thermal initiated radical polymerization and it can be prepared at any temperatures. Another significant advantage is a greater penetration depth of ionizing over polymerization. Thus, a monolith can be prepared at any desirable sizes [23]. Additionally, the thermal initiated polymerization is difficult to assign the polymerization space precisely. The principle of the UV polymerization is similar to the photolithography patterning as the reaction can occur within the specified area exposed through a mask.

The most common monolithics are base on polystyrenes, polymethacrylates and polyacrylamides. Both methacrylate and styrene based monoliths are most often prepared as hydrophobic monoliths for example glycidyl methacrylate(GMA) , ethyl dimethacrylate (EDMA) and buty methacrylate (BuMA). The generally monomers for polymerization are GMA and EDMA which are often used as a starting point for future functionalisation of monolith , due to the surface can be modified. The high reactivity of the epoxy ring in GMA allows the ring to be opened to create a negatively charged on surface. This can be further functionalized for example Potter et al. have modified a poly (GMA-co-EDMA) monolith by flushing with p-hydroxyphenylboronic acid to allow the phenylboronic acid stick onto the surface. The attached phenylboronic acid sites can be used to retain carbohydrates through their 1, 3 -cis-vicinal diol groups [24]. Dong et al. have prepared a zwitterionic stationary phase by taking a poly (GMA-co-EDMA) monolithic scaffold, filling the pores with a solution of lysine, which attack the epoxy ring and bind to the surface creating a stationary phase which can be cationic or anionic depending on the pH of the environment [25].

The porogenic solvent is the one of the essential parts for the polymerization. There are two main objectives of the porogenic solvent which are: (i) to dissolve all monomers and initiator to create a homogeneous solution and (ii) to control the separation during the polymerization to reach the desired pore structure [26]. The composition of the porogenic mixture is designed to control the flow resistance of the device. Moreover, the porosity of the monolith could be controlled by adjusting the composition and the percentage of the porogenic solvent. It was found that alcohol as a porogenic solvent leaded to big pore size while a solvent like acetone, ethylpropionate, and dioxane caused very small pores in a monolith [27]. Some research studies reported that the pore size was also a function of the monomer concentration, the type of solvent, the total adsorbed dose, and the synthesized temperature. An increase in the monomer concentration also results in smaller pores. Although the small pore size monolithic polymer provides a large surface area for adsorption, it requires high pressure to pass fluid through. Hence, it is useless in a flow application.

Rohr et al., [28] found cyclohexanol and 1- decanol to be the most efficient porogenic solvent among other solvents tested. An increase in the percentage of 1-decanol resulted in an increase in the monolith's pore size. However, the mixture was not suitable to synthesize the monolith with pore larger than 1 μm from monomers of HEMA and EDMA. In addition, they studied the effect of various initiators on the polymerization duration. There were 2 interesting initiators which were azobisisobutyronitrile (AIBN) and 2, 2-dimethoxy-2-phenylacetophenone (DAP). AIBN caused a slower polymerization than DAP. AIBN took approximately 90 minutes to complete the polymerization while DAP required only 10 minutes because of its rapid induction of a free radical reaction.

2.3Modification of monolith

The modification of stationary phase chemistries is generally carried out to change the selectivity of the phase. This may be to take advantage of certain characteristics of one stationary phase and apply them to different mode of chromatography**.**

2.3.1Chemical modification

For permanent modification of stationary phase chemistry the formation of chemical bonds is required. The modification is generally carried out on-column. Sugrue et al. modified the surface of both particle and silicabased monolithic columns with iminodiacetic acid (IDA). The modification was facilitated by the reaction of the epoxy group with the nitrogen of the IDA molecule, and the reaction of the silane group with the bare silica of the column. The columns were then suitable for the analysis of transitionmetal cations. The monolithic column was found to yield faster more efficient separations when using high ionic strength eluents compared to the particle based column). Using the same functionalisation methodology Sugrue et al. functionalised a silica monolith with lysine for the separation of both anions and cations on one stationary phase. This was possible as lysine once bonded to the silica monolith will act as a zwitterionic stationary phase .

The use of epoxy group reactivity to functionalise stationary phases has been used widely in conjunction with glycidyl methacrylate (GMA) based monoliths. Figure 2.4 depicts a selection of functionalities created using epoxy groups on the surface of GMA monoliths.

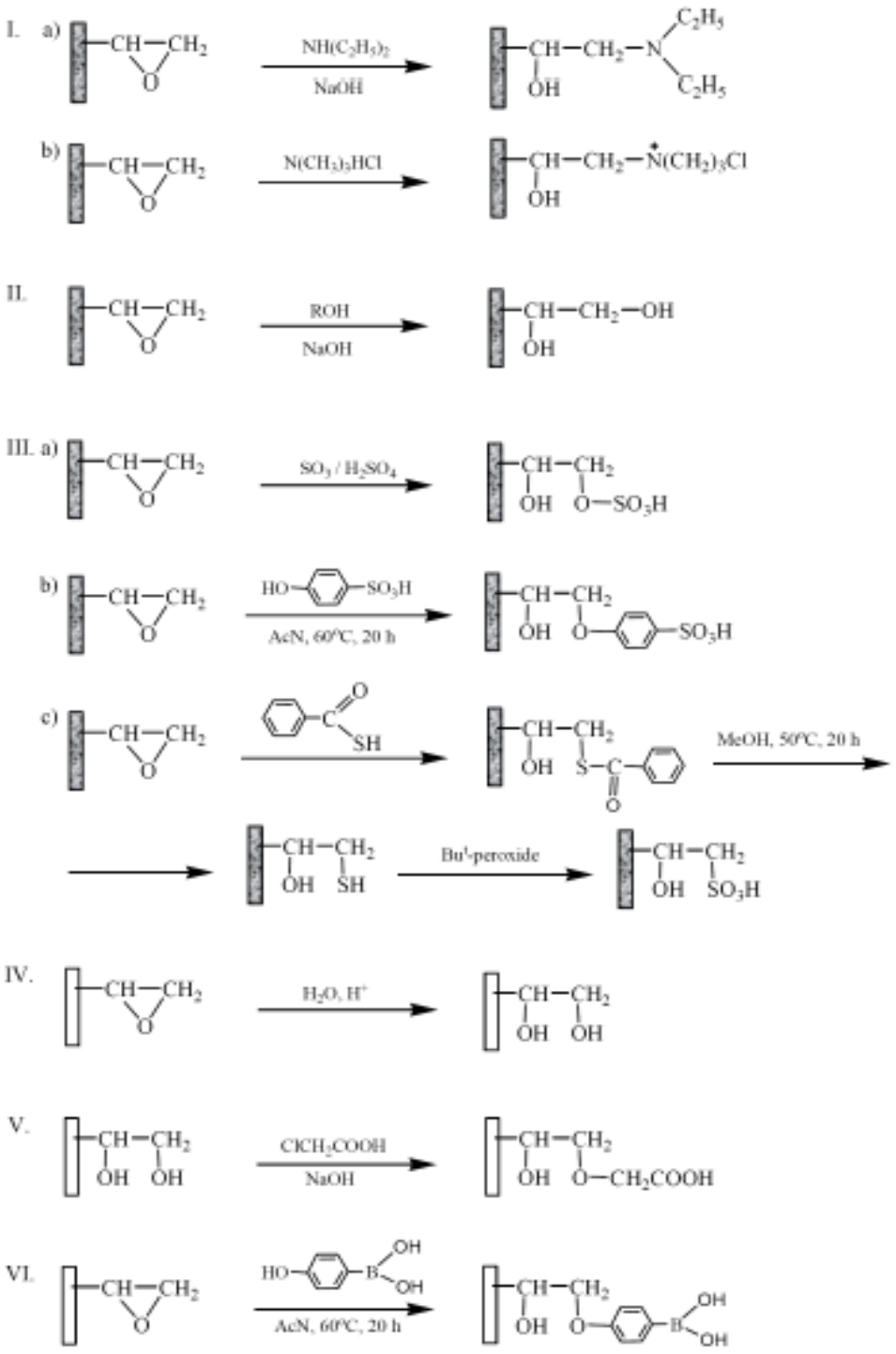

Figure 2.4 Chemical conversion of epoxy groups by means of various reagents.
I. Amination; II. alkylation; III. sulfonation; IV. hydrolysis;
V. carboxymethylation; VI. modification with p-hydroxyphenylboronic acid.

Preinersfer, et al. [3], modified the epoxy groups of a poly(GMA-co-EDMA) monolith in such a way that the reactive thiol group are generated which can be untilized to attach a chromatographic ligand in a second step by versatile chemistries, e.g. by radical addition, graft polymerization, nucleophilic substitution, disulfide formation and Michael addition reaction. The existing epoxide groups on poly(GMA-co-EDMA) were transformed to 3-mercapto-2-hydroxy-propyl residues in a nucleophilic substitution reaction, employing sodium-hydrogen sulfide in aqueous media as nucleophilic reagent as can been see in Figure 2.5.

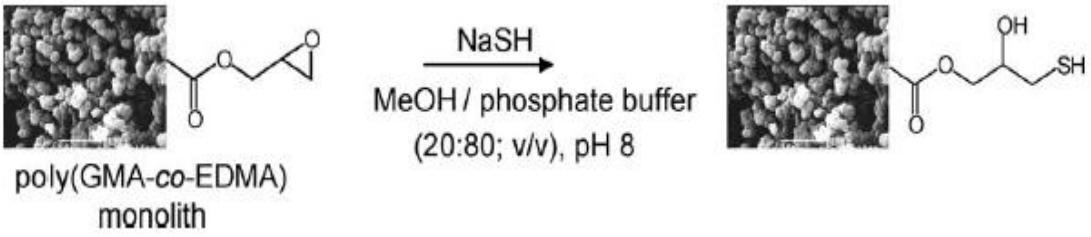

Figure 2.5 Reaction scheme of surface modification for the preparation of reactive thiol monoliths [3].

2.4 Cysteine

Cysteine is one of the most important biogenic amino acids with formula structure $O_2CCH(NH_2)CH_2SH$ which linked by peptide bonds form polypeptides and proteins. The side chain on cysteine is thiol group (SH), which is nonpolar and thus cysteine is usually classified as a hydrophobic amino acid. The thiol is susceptible to oxidization to give the disulfide derivative cystine. The following figure is a chemical structure of cysteine [29-30].

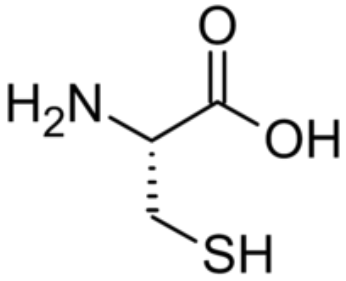

Figure 2.6 chemical structure of cysteine [30].

The thiol groups of cysteine are formed disulfide bonds in proteins by oxidation reaction. The other sulfur-containing amino acid methionine, cannot form disulfide bonds . More aggressive oxidants convert cysteine to the corresponding sulfinic acid and sulfonic acid. This reaction is reversible, and a mild reduction cleaves the disulfide [30].

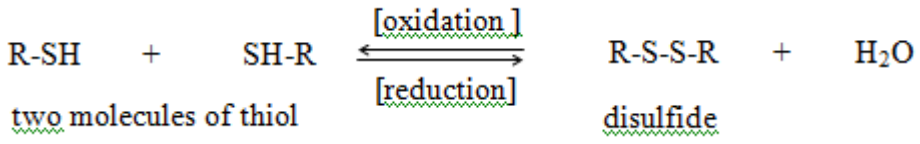

Inside the cell, disulfide bridges between cysteine residues within a polypeptide support the protein's tertiary structure. Insulin is an example of a protein with cystine crosslinking, wherein two separate peptide chains are connected by a pair of disulfide bonds.

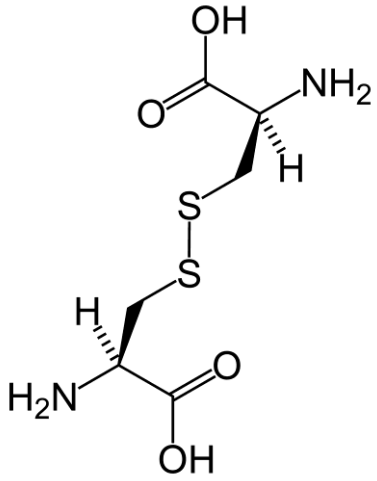

Figure 2.7 chemical structure of cystine.

The reasons why cysteine is important are shown as follows:

(i) It has a very reactive thiol group at its side chain. This leads to a special position that cannot be replaced or substituted by any other amino acid.
(ii) Disulfide bridges formed by cysteine residues are permanent components of protein primary structure.
(iii) It can change its secondary structure by steric constraints.
(iv) Cysteine is at the center of the catalytic site of thiol enzymes.
(v) It is an essential unit of the low molecular weight factors in the overall redox potential in the biological systems.

Generally, cysteine is unstable. It is easily converted to cystine and thus cysteine is adsorbed in human body in terms of cystine. Some studies reveal that cysteine and cystine behave as a strongly hydrophobic residue in a globular protein. The hydrophobicity of cysteine seems to conflict with the polarized behavior of the thiol group. However, it is considered that the thiol group is inactive in water molecules. The thiol group has no ability to form a hydrogen bond with water. This can explain why the thiol group is hydrophobic in water [31].

2.5 Adsorption process

Adsorption is a process that involves the accumulation of molecular or the concentration on the surface or the interface. This process can occur between the liquid and liquid, gas and liquid, gas and solid or solid and liquid. Adsorption process involves two components adsorbent and adsorbate. Adsorbent is the substance on the surface of which adsorption takes place. Adsorbate is the substance which is being adsorbed on the surface of adsorbent. Adsorption processes can be classified in to two type which are physical adsorption and chemical adsorption depending on type of forces of attraction existing between adsorbate and adsorbent [37-38].

Physical adsorption is the result of relatively weak Van der Waal's interaction forces between the solid surface and the adsorbate a physical attraction. Physical adsorption is easily reversed. Depending on the gas and solid, the adsorption phenomenon also can result in the sharing of electrons between the adsorbate and the solid surface. Chemical

adsorption or chemisorptions is result from chemical bonding between adsorbate and adsorbent that it unlike physiorption, chemisorption is difficult to reverse. A significant quantity of energy usually is required to remove chemically adsorbed molecules [39].

Paul A. Webb., [40] physical adsorption takes place on all surfaces provided that temperature and pressure conditions are favorable. However, chemisorption occurs only between certain adsorbents and adsorptive species and only if the surface is cleaned of previously adsorbed molecules. Under suitable conditions, physical adsorption can result in adsorbed molecules forming multiple layers while chemisorption occurred only proceeds as long as the adsorptive can make direct contact with the surface. It is a single-layer process. A chemically adsorbed molecule is strongly bound to the surface and cannot escape without the influx of a relatively large quantity of energy compared to that necessary to liberate a physically bound molecule. This energy is provided by heat and often very high temperatures are required to clean a surface of chemically adsorbed molecules.

Adsorption is present in many natural physical, biological, and chemical systems, and is widely used in industrial applications such as activated charcoal, capturing and using waste heat to provide cold water for air conditioning and other process requirements (adsorption chillers), synthetic resins, increase storage capacity of carbide-derived carbons for tunable nanoporous carbon, and water purification. Adsorption, ion exchange, and chromatography are sorption processes in which certain adsorbates are selectively transferred from the fluid phase to the surface of insoluble, rigid particles suspended in a vessel or packed in a column. Lesser known, are the pharmaceutical industry applications as a means to prolong neurological exposure to specific drugs or parts of there [41].

2.6 Reducing agent

Reagent that reduce disulfide group are useful for purpose of (i) reducing native agent disulfide groups and (ii) maintaining thiol groups in solution by preventing their oxidation to disulfide state. Dithotheritol(DTT) is the most popular reagent used presently in biochemistry for reduction of disulfide groups[42]. However, DDT is slow in reduction disulfide groups at pH 7 to 8, because of its high value of pKa. It is expensive Due to mercaptoethanol is inexpensive, it can be used in large amount in biochemical manipulation. The pKa of mercaptoethanol is 9.6[43]. The disadvantage of mercaptoethanol is weak reducing agent and foul-smelling. It often generated complex reaction mixtures containing mixed disulfide [44].

In an earlier account, Levison et al. reported the use of two water-soluble phosphines, tris-(hydroxymethyl) phosphine and tris-(2-carboxyethyl) phosphine (TCEP) for the reduction of human gamma-gamma-globulin [45]. Tris(2-carboxyethyl) phosphine (TCEP) is widely employed as a reductant of disulfide bonds in a variety of peptide, protein, and cellular systems. Model studies show that reduction of disulfides by phosphines is initiated by rate-limiting formation of a thiophosphonium salt.Subsequent, rapid, hydrolysis releases the second thiol fragment and the phosphine oxide [42].

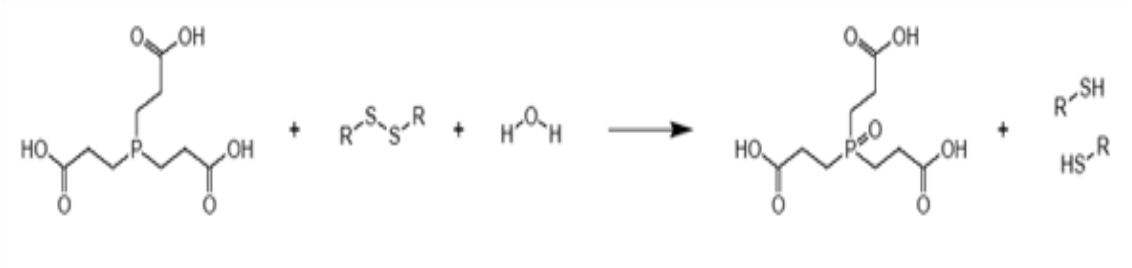

Figure 2.8 Disulfide reaction by phosphine [47]**.**

TCEP provides a particularly useful complement to dithiothreitol (DTT) because the phosphine is comparatively air-stable, and an essentially irreversible reductant of disulfide bonds. Unlike oxidized DTT, oxidized TCEP cannot directly catalyze thiol-disulfide exchange reactions, and this, together with its superior reactivity at low pH values, has made it the reagent of choice for a number of biochemical applications [46].

TCEP selectively and completely reduces even the most stable water-soluble alkyl disulfides over a wide pH range. Reductions frequently require less than 5 minutes at room temperature. TCEP is non-volatile, odorless, and unlike most other reducing agents, is resistant to air oxidation. Compared to DTT, TCEP is more stable, more effective, and able to reduce disulfide bonds at lower pH [47].

Advantages of TCEP over traditional alternatives for reducing disulfides:

- Odorless – Unlike DTT or BME, TCEP is odor-free, so reductions can be carried out conveniently on the bench top.
- Stable in air – The inherent stability of the TCEP moiety eliminates the need for any special precautions to avoid oxidation when handling, using or storing TCEP.
- Efficient – For most applications, 5-50 mM TCEP provides sufficient molar excess to effectively reduce peptide or protein disulfide bonds within a few minutes at room temperature.
- Compatible – With TCEP, removal of the reducing agent is not necessary prior to most applications, (e.g. histidine-tagged protein purification, maleimide conjugations).

2.7 Previous Research

Since this project is continued from the previous research "Development of microfluidic sample preconcentration system for cysteine uses BuMA-EDMA" by Archiraya [6], it is necessary to review the previous research. Similar to our project, Archiraya examined the method for fabrication of microfluidic channel from PDMS mixer on glass slide. The monolithic polymers are BuMA and EDMA in porogenic solvent of cyclohexanol and 1- decanol. The initiator for the UV photoinitiated polymerization is DAP. The interesting parameters for the characterization of monolithic concentrator were the monomer concentrations, the polymerization duration, and the flow rate of the liquid sample. Scanning Electron Micrograph (SEM) and BET pore size analysis were used to investigate the morphology of the monolithic polymer. SEM was used to determine the polymer bead size, the dimensions of macropores (irregular voids between these clusters) and mesopores (the pores between the individual polymer beads) while BET

was used to verify the size of the micropores (the pore within the polymer beads) and surface area.

Initially, the researcher studied the effect of monomer concentration and polymerization duration on the morphology of monolith by varying the monomer concentration (12.5 % , 25 % ,50% and 75% by weight monolithic) and different UV exposure time (10, 20 and 30 min). The characterizing use Scanning Electron Microscope (SEM) and BET for structural analysis. The results show that the monolith polymerized from a higher monomer concentration using longer polymerization time possessed higher surface area with smaller micropore and bead size. However, the 75-percent-by-weight-monolith resulted in very large flow resistance. A balance must be found between the requirements of low flow resistance and high surface area. Therefore, the monolith prepared with 50-percent-by-weight-monomer concentration polymerized for 30 min was chosen for the preconcentration study.

After completing the synthesis of the monolithic polymer in the microchannel, the sample preconcentration would be examined by using cystiene in aqueous solution as a liquid sample to determine the optimum flow rate and adsorption efficiency. The preconcentration would be carried out after eluting the accumulated cystiene inside the monolith with 0.1 M H_2SO_4. The optimum flow rate was verified by varying the flow rate of cystiene solution between 5 – 20 µl/min. The results were shown in terms of fold increasing in cysteine adsorption. It was found that the amount of cystiene adsorbed on the monolith surface increased when increasing the flow rate from 5 to 10 µl/ min, a greater amount of cysteine accumulated was obtained. This was caused by larger amount of cysteine fed through the monolithic polymer resulting greater mass transfer between the monolith and the bulk sample. However, when the feed rate of the cysteine sample increased from 10 to 15, and 20µl/min, a decrease in the adsorption efficiency was observed. This was resulted from the less contact time between cysteine and the monolith. The maximal amount or efficiency of cysteine adsorption onto the monolith was found to be 35.9 % when the system was operated at 10µl/min. The researcher also examined the adsorption efficiency by varying the concentration of cystiene was varied between 0.1-10 millimolar. The results show the adsorption efficiency increased as the concentration of cysteine raised from 0.1-1 millimolar. In contrast, an increase in cysteine's concentration from 1 to 10 millimolar resulted in a decrease in the adsorption efficiency from 35.60 to 17.67 % This was caused by the saturation of the surface area for the mass transfer in the monolith. Consequently, the best condition for the adsorption was obtained using the feed flow rate at 10 µl/min and inlet concentration at 1 millimolar. Cysteine adsorbed on the monolith was then eluted by using 0.1-molar-sulfuric acid. The maximal fold increase was 5.74 when the elution rate was at 5 µl/ hr for 2 hours.

In the previous research mentioned earlier leads to the motivation of our project "Preconcentration of Cysteine in Microfluidic channel". The differences between our project and the previous research are the monolithic monomer and porogenic solvent. We should develope the adsorption efficiency of monolithic by generating the reactive thiol groups on poly (GMA-co-EDMA) monolithic in a nucleophilic substitution reaction by using sodium-hydrogen sulfide (NaSH) as necleophilic reagent. We hope that thiol groups are able to occur disulfide formation with cysteine. Resulting from bonding between disulfide formations, the adsorption efficiency will increase.

CHAPTER 3 METHODOLOGY

3.1 Materials

- Glass capillary tubes with 1mm in diameter
- Methacrylate monomer, the combination of glycidyl methacrylate and ethylene dimethacrylate (EDMA) mixed at 3:2 ratio with a monomer concentration of 12.5, 25, and 50% by weight
- Porogenic mixture consisting of equal volumes of methanol and ethanol.
- 2,2-dimethoxy-2-phenylacetophenone (DAP) as an initiator
- Cysteine in aqueous solution
    - 2 M of sodium-hydrogen sulphide (NaSH) (Sigma-Aldrich)
    - 2,2' dipyridyldisulfide in acetone
- tris (2-carboxyethyl) phosphine hydrochloride (TCEP) as an eluent

3.2 Monolith Concentrator

3.2.1 Preparation of Monolith Concentrator

The monomer mixture was prepared by mixing GMA and EDMA at 3:2 mass ratio in a porogenic solvent, consisting of methanol and ethanol (1:1 by volume). The 2,2-dimethoxy-2-phenylacetophenone (DAP) was added to the solution as an initiator (1% wt monomer) which was chosen for this study because of its high reactivity even with low intensity UV light. Afterwards, the mixture was sonicated for 10 min, followed by purging with nitrogen for 5 min to remove dissolved oxygen. The polymerization mixture was introduced to a glass capillary tube. The concentration of the monomer mixture was varied between 12.5, 25, and 50% to study the effect of the monomer concentrations on the monolithic structure which will be described in details in the next topic.

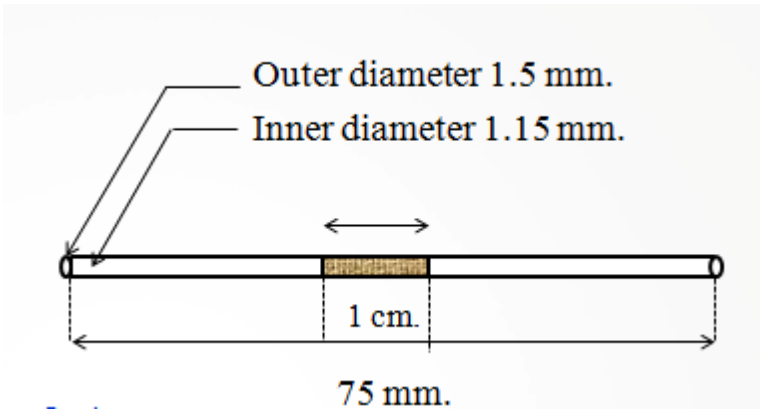

Figure 3.1 The dimension of glass capillary tube.

A glass capillary tube was filled with the polymerization mixture using a syringe pump and the glass capillary tube was covered with a mask containing small rectangular transparent area to allow for UV exposure at the desired position about 1 centimeter in length. The glass capillary tube was placed at a distance of 2-3 cm away from the UV light source (Atman, 365-nm18-Watt 240-Volt UV lamp). The in situ polymerization proceeds for either 10, 20 or 30 minutes at room temperature. The resulting monolith was rinsed with methanol using a syringe pump. The polymerization time, another interesting parameter, was varied to determine the optimum condition.

Table 3.1 Compositions of the polymerization mixture in weight percent.

Composition	Polymer 1	Polymer 2	Polymer 3
	12.5 wt %	25 wt %	50 wt %
GMA	7.5	15	30
EDMA	5	10	20
Ethanol	43.75	37.5	25
Methanol	43.75	37.5	25
DAP	1	1	1

3.2.2 Preparation procedure for thiol-monolith

A 2 M solution of sodium-hydrogen sulfide was freshly prepared by dissolving it in a mixture of 0.1 M aqueous sodium dihydrogenphosphate in methanol 20:80 (v/v) and sonicating it for a few minutes. Afterwards the solution was filtered through a nylon membrane filter. The pH was adjusted to 8.15 with diluted orthophosphoric acid. Before surface modification, the monolith was rinsed with methanol–water at the ratio 20:80 (v/v) employing a syringe pump. The glass capillary tube was then flushed with 60 µl of the sodium-hydrogen sulfide solution using a syringe and a syringe pump at a flow rate of 30 $\mu l h^{-1}$. After 2 hours, the glass capillary tube was attached to a syringe pump and rinsed with methanol–water 20:80 (v/v).

3.2.3 Quantitative determination of the generated thiol groups on the monolith surface

The amount of thiol groups were determined using a disulfide exchanger reaction with excess dipyridyldisulfide (DPDS) at room temperature. For determination of generated thiol, 1.19 M solution of 2, 2’ dipyridyldisulfide in acetonitrite was filled into the capillary. The disulfide exchange reaction was allowed to occur for 1 hour. Subsequently, the capillary tube was rinsed with acetonitrile for 35 min. The reaction produced pyridine-2-thione and non-reacted DPDS was separated. Pyridine-2-thione was detected at a wavelength of 440 nm, while the excessive reagent was detected at 254 nm.

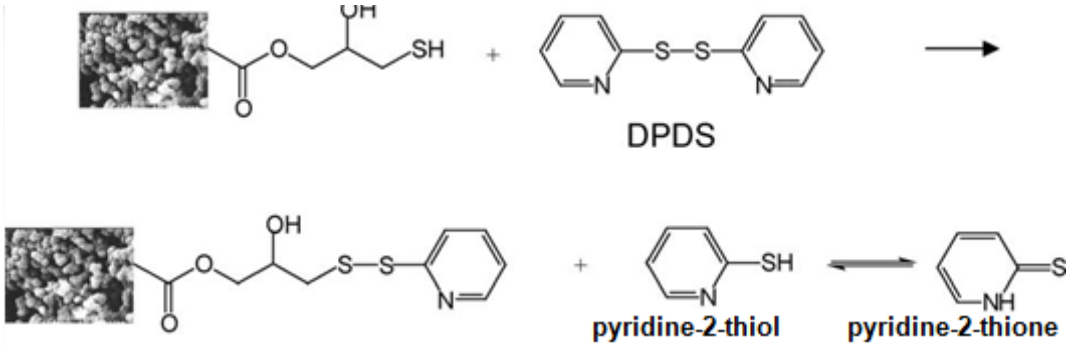

Figure 3.2 Reaction scheme for the quantitative dtermination of thiol groups on the monolith surface using DPDS as a chromogenic reagent [3].

A calibration curve was established using a monolith with non-modified epoxy group. The standard solution was prepared by mixing DPDS with different amounts of 2-mercaptoethanol (Sigma-Aldrich). The reaction was allowed to occur for at least 1 h at room temperature.

3.3 Characterization of Monolithic Concentrator

There were 2 significant parameters that affected the properties of a monolith concentrator. They were the monomer concentration of the mixture and the polymerization duration. The polymerization time was varied between 10 to 20 and 30 minutes while keeping the monomer concentration constant to determine the optimal polymerization time. In order to study the effect of the monomer concentration on the morphology of the monolithic, the monomer concentration of GMA and EDMA at 3:2 in mass ratio was changed between 12.5, 25, and 50 wt %.

Scanning Electron Microscope (SEM, JSM-5800) was used to determine the morphology of monolith, the pore structures of the polymerized monolith and, portions of the synthesized monoliths at various conditions. BET (Autosorb 1, Quantachrome Corporation) surface analysis was used to determine the pore sizes and the surface areas. In addition, Scion Image analysis (version 4.03 from Scion Corporation) was carried out for the estimation of their void fractions and average bead size.

Following the variation in the monomer concentration and the polymerization time, the liquid flow rate was fed to the tube after polymerization, the pressure drop across the channel or the flow resistance became the significant parameter. The pressure needed to drive the liquid through any system should be as low as possible. In this study, the preconcentration is involved in an adsorption process and associated with a mass transfer between bulk phases to pores inside each polymer beads. As a result, the most significant parameter for preconcentration process is the pore size. Pore sizes could represent surfaces area for the mass transfer. Smaller pores provide greater surface areas; however, they also cause a higher flow resistance.

3.4 Sample Preconcentration

After the monolithic polymerization, the glass capillary tube was connected to a syringe pump in order to feed a fluid including the liquid sample (dilute cysteine in deionized water) into the device through an inlet hole. Afterwards, the sample consisting of 0.3 millimolar cysteine was injected at a flow rate of 10 μL/min for 90 min. Cysteine was adsorbed on polymeric beads within the monolithic concentrator while the rest of sample flowed through. To determine the amount of cysteine accumulated, the material balance was applied by analyzing the different quantity of cysteine at the inlet and outlet. Thus, the liquid outlet was collected to measure the amount of cysteine adsorbed on the monolith and determine its adsorption efficiency. Cysteine accumulated in the channel was eluted using 10 μl of tris (2-carboxyethyl) phosphine hydrochloride (TCEP). The concentration of cysteine eluted was measured using UV-spectrophotometer (U-3000) at 232.5 nm.

The performance of the monolithic concentrator was determined based on an increase in cysteine concentration. To obtain a suitable operating condition for the preconcentration system, several parameters, for example inlet flow rate, elution rate and concentration of cysteine in the inlet flow, were investigated. Initially, the feed flow rate of the sample consisting of 0.3 millimolar cysteine was 10μL/min. Afterwards, the concentration of

cysteine were varied between 0.05 – 1 millimolar at the optimal flow rate for 90 min. Finally, the effect of the eluent flow rates, in the range of 3-10 μL/hr, on the outlet concentration of cysteine was investigated. In this experiment, the volume of the eluent was maintained at 10 μL. Therefore the elution duration had to be prolonged for lower flow rates. Table 3.2 demonstrates the elution durations and the elution rates at the controlled volume of 10 μL.

Table 3.2 Elution durations and elution rates at the controlled volume of 10-μL for the preconcentration study.

Elution rate (μL/hr)	Elution time (min)	Volume of elution (μL)
3	200	10
5	120	
10	60	

CHAPTER 4 RESULTS AND DISCUSSION

4.1 Monolith Concentrator

From Kanthiya's study, the monoliths from that study were homogeneously filled the entire capillary while Achiraya's study showed that there was a gap between the monolith and the wall. This demonstrates the difference in the capillary wall thickness and the PDMS microchannel thickness which may have contributed to the difference in the monolithic morphology. The capillary wall is much thinner than that of the microchannel, allowing for higher UV intensity for polymerization. In addition, PDMS also absorbed UV light in itself. Therefore, UV penetration through the microchannel was significantly less, as compared to the capillary which did not absorb UV. Therefore, the glass capillary tube was chosen for the preliminary experiments.

4.1.1Preparation of monolith concentrator

The monolithic polymer was prepared from a polymerization mixture consisting of glycidyl methacrylate (GMA) as a monomer and ethylene dimethacrylate (EDMA) as a crosslinker at 3:2 mass ratios. The proposed structure of the GMA-EDMA copolymer is shown in Fig.4. 1.

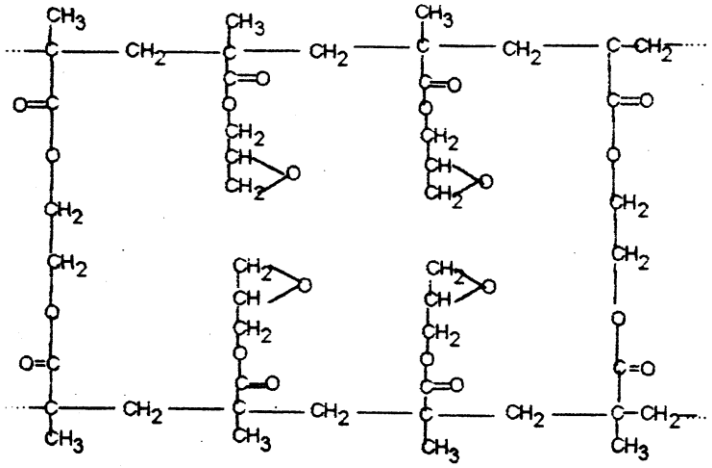

Figure 4.1 Structure of GMA-EDMA copolymer [39].

Both polymers were dissolved in porogenic solvent, which were methanol and ethanol. The polymerization was started by exposing the polymer soluiton to UV-light though decoposition of DAP which was added as an initiator. The mass ratio of GMA and EDMA is 3:2 was selected from the previous work. Camilla and cowoker [43] studied the effects of the concentration of cross-linking monomer in the polymerization mixture and composition of the porogenic solvent on the porous structure obtained with the two chemically different systems of styrenic and methacrylate monomers. The experiments with monomer mixtures containing 40% and 60% ethylene dimethacrylatethe resulted in the pore size distributions shift to smaller pore sizes as the percentage of cross-linker increased. However, the resistance to flow is also an important issue and the pressure needed to drive the liquid through the monolith should be as low as possible and highest possible content of a functionalized monovinyl monomer was required. Consequently, 40% of ethylene dimethacrylatethe is proposed to be a suitable ratio.

The monolithic polymer was successful synthesized inside a glass capillary tube by the UV-initiated polymerization reaction, as illustrated in Figure 4.2.

Figure 4.2 The glass capillary filled with 25 wt % monomer before polymerization.

After UV-initiated polymerization, the polymer chain formed in the solution as soon as they became insoluble in the reaction medium either as a result of the cross-linking density of the polymer network, or the porogenic agent used [22]. Figure 4.3 shows the formation of the monolith in glass capillary tube.

Figure 4.3 The glass capillary filled with 25 wt % monomer after polymerization.

According to Figure 4.2 and 4.3, the polymerization mixture before UV-polymerization was transparent. Once polymerized, the polymer appeared opaque in the specified area in less than 10 minutes.

The aim of this study is the preconcentration of cysteine by chemisorption on the surface of the monolith polymer. The adsorbed surface area is an important factor that affects to adsorption mechanism. The monolithic polymer should have high surface area in order to achieve greater exposure of functional groups, resulting in an increase in the

yield of a good binding capacity. Thus, smaller pores would be desired in monolithic polymer. However, the monolithic polymer must have enough porosity to allow liquid to flow through at low pressure [22]. The monolith which has high surface area would likely cause high flow resistance or pressure drop across itself. To balance between required low pressure drop and high surface area. The monolithic polymer contains large pores size suitable for liquid transport. However, smaller pores provide a good binding capacity, albeit high back pressure. High back pressure would retard the flow through the porous polymer and can possibly cause leakage between the tube and the inlet port. As a result, the back pressure, then, became the parameter which must be determined.

Therefore, the morphology and porous structure of the monolith were investigated in this study. Important parameters that directly affected the morphology and porous structure of monolith included monomer concentrations (12.5, 25, and 50%wt) and polymerization durations (10, 20, and 30 minutes).

From the preliminary experiment, it was found that 12.5% wt of monomer mixture was opaque in glass capillary tube after UV-polymerization for 10, 20, and 30 minutes. Unfortunately, they were not uniformed and less attached to the surface of the glass capillary tube. Numerous voids between the wall surface and the monoliths occurred. It is possible that there were only a small amount of the monomers available to be cross-linked with each other and attached to the wall [3]. Twenty five and 50% wt of monomer mixture were opaque in the glass capillary tube and uniform at all duration polymerization, indicating a complete conversion. Consequently, the monolith prepared from 12.5% wt monomer mixture was not chosen for further experiments.

The morphology and porous structure of monolith were investigated by Scanning Electron Microscope (SEM). Moreover, Scion Image Analysis was used to determine the particle size and void faction of monolith. Scion Image Analysis is an image processing and analysis program. It can be used to measure area, mean, perimeter, centroid, etc. of user defined region of interest. The morphologies resulting from SEM was shown in Figures 4.4-4.9. The monolith was synthesized at different concentrations of monomer mixture and polymerization time.

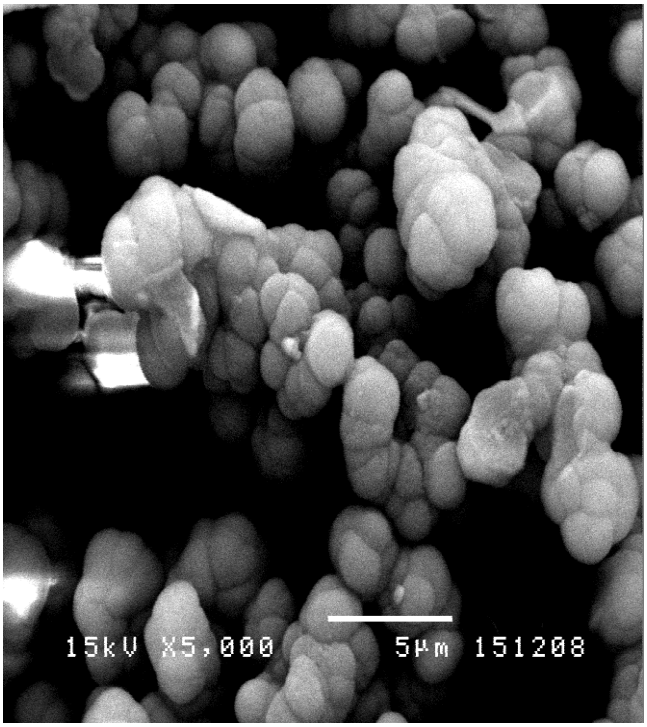

Figure 4.4 SEM micrograph of the cross sectional monolith in the capillary tube (x5,000) prepared by 25 wt % monomer and polymerized for10 min

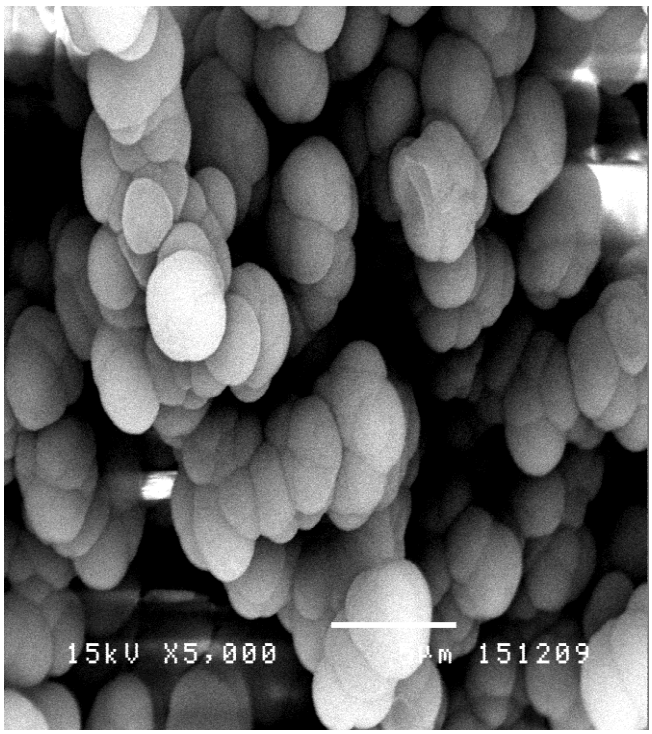

Figure 4.5 SEM micrograph of the cross sectional monolith in the capillary tube (x5,000) prepared by 25 wt % monomer and polymerized for 20 min

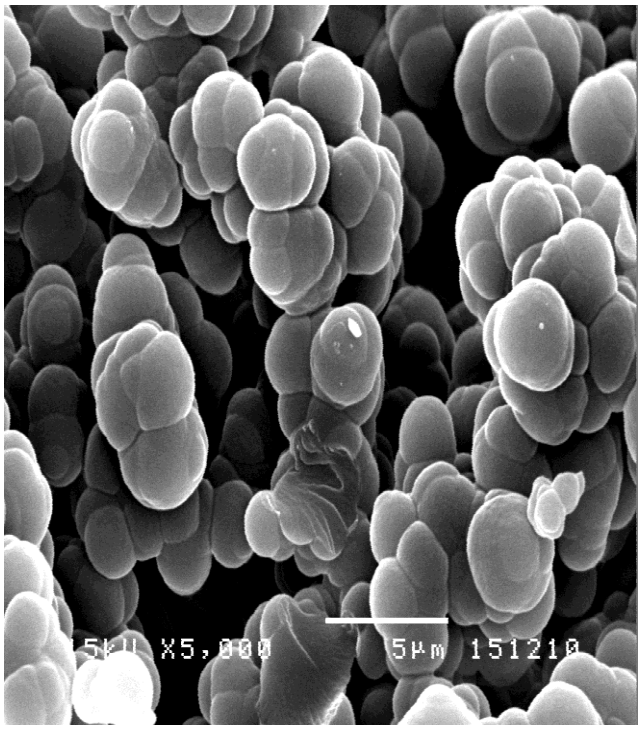

Figure 4.6 SEM micrograph of the cross sectional monolith in the capillary tube (x5,000) prepared by 25 wt % monomer and polymerized for 30 min

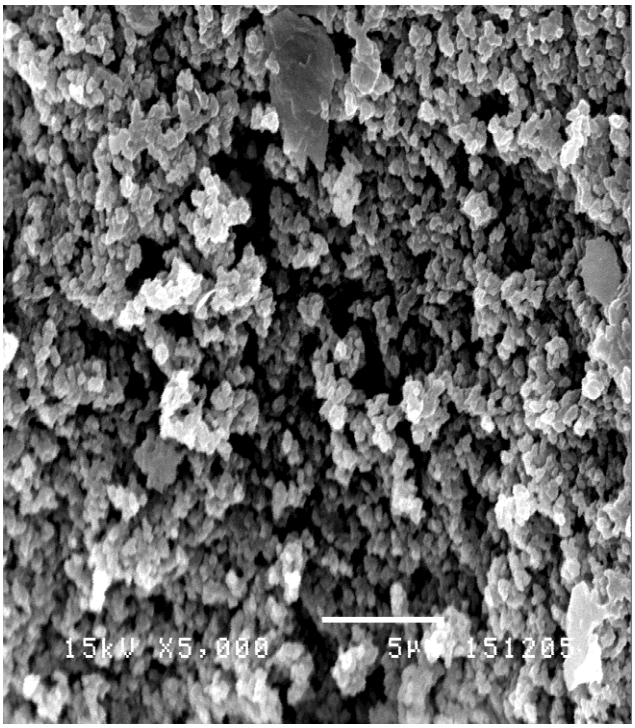

Figure 4.7 SEM micrograph of the cross sectional monolith in the capillary tube (x5,000) prepared by 50 wt % monomer and polymerized for 10 min

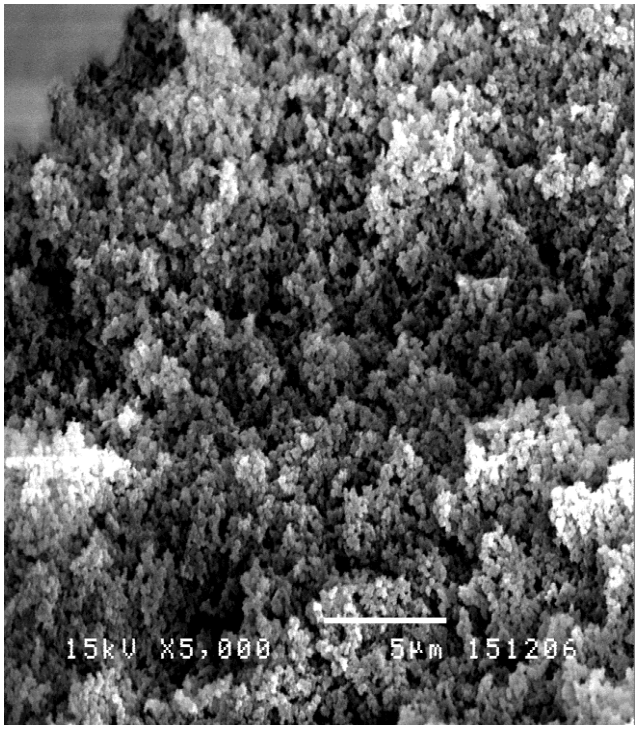

Figure 4.8 SEM micrograph of the cross sectional monolith in the capillary tube (x5,000) prepared by 50 wt % monomer and polymerized for 20 min

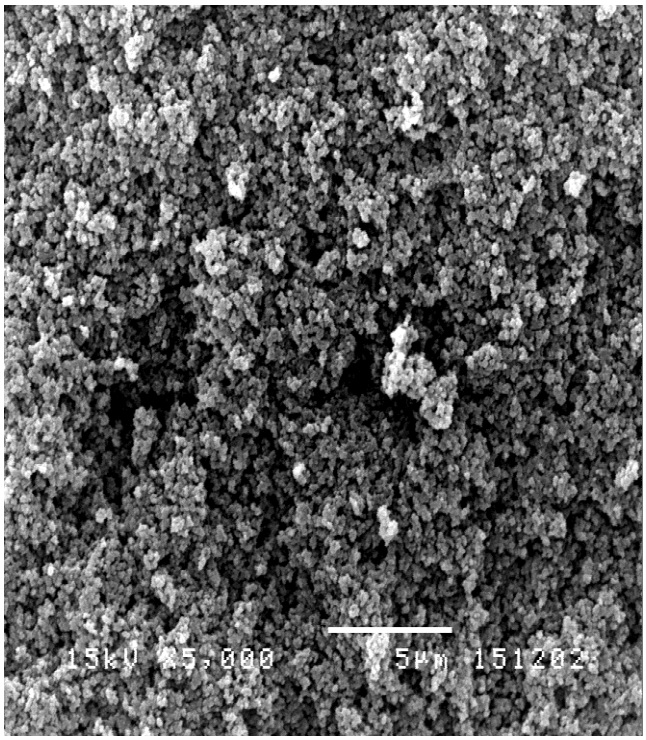

Figure 4.9 SEM micrograph of the cross sectional monolith in the capillary tube (x5,000) prepared by 50 wt % monomer and polymerized for 30 min

According to Figures 4.4 - 4.9, different concentrations of monomer mixture and polymerization time affected the particle and pore size of the monolith. The monolith contains three types of pores which are macropores with large pores that allow the liquid flow through and mesopores refer to pores between 2 to 50 nm in diameter followed by micropores with pore diameter smaller than 2 nm. Both of the micropores and the mesopores have significantly contributed to the overall adsorbed surface area while the macropors has a negligible effect on the adsorption [32]. In the preconcentration, high flow rates are required in order to accommodate very dilute samples. The monolith with the large pores allows high flow rates but typically has limited surface areas which affect the adsorption mechanism. Therefore, the criteria for choosing the best monolith are smaller pore for high surface areas and low flow resistant.

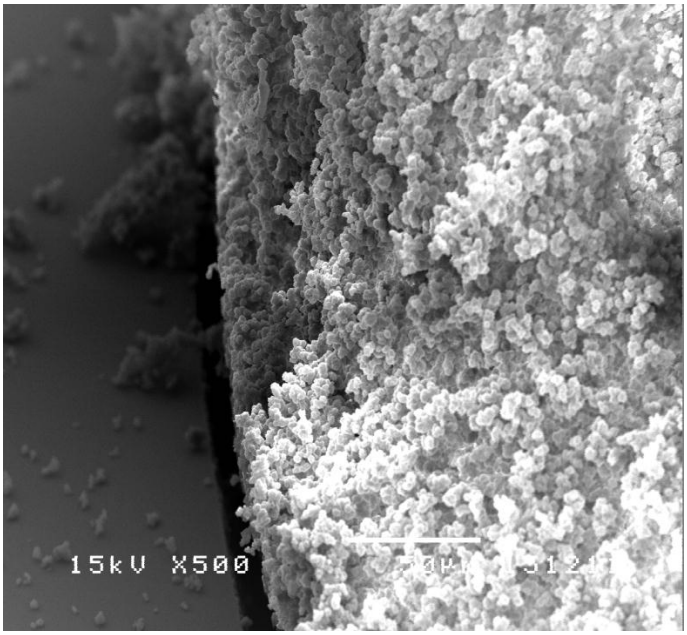

Figure 4.10 SEM micrograph between monolith and the capillary wall.

The SEM micrograph illustrated that there was a gap between the monolith and the wall as shown in Figure 4.10 .The monolith was poorly attached with the inner wall of capillary tube. Because of the glass capillary tube is the hydrophilic while the GMA-EDMA monolith is the hydrophobic so that capillary pretreatment procedure should be carried out in order to enhance the covalent attachment of GMA-EDMA monolith to the capillary wall [3]. For another reason, the capillary tube was damaged from cutting the sample for SEM visualization causing the crack lead to a gap between the monolith and capillary wall.

4.1.1 Effect of Monomer Concentrations

The morphology of the monoliths is controlled by the quality of the porogen solvent, the concentration of the monomer, the ratio between the monomer and the porogen phases, and the polymerization temperature and time [36]. Thus, in this study, we investigated the effect of monomer concentration and polymerization time that directly related to the morphology and pore size. From SEM micrographs of the monolith at various conditions, we used Scion Image Analysis program to estimate the average bead size

and void fractions. The monoliths polymerized at 25 and 50 % wt monomer in porogenic mixture at 10, 20 and 30 minutes were the samples to study the effect of the monomer concentration on the particle size and void fractions, as shown in Table 4.1.

Table 4.1 Bead size and void fraction of monoliths were prepared at various conditions.

Monoliths prepared by	Average length of bead (μm)	Void fraction
25 wt % 10 min	1.91 ± 0.210	0.62
25 wt % 20 min	1.876 ± 0.185	0.56
25 wt % 30 min	1.818 ± 0.162	0.52
50 wt % 10 min	0.250 ± 0.100	0.41
50 wt % 20 min	0.224 ± 0.036	0.38
50 wt % 30 min	0.193 ± 0.026	0.33

According to Table 4.1, the largest bead size was observed in the monolith with 25% wt monomer concentration polymerized for 10 minutes and the smallest bead size was observed in the monolith with 50% wt monomer concentration polymerized for 30 minutes. When keeping the polymerization time constant at 10 minutes, the monolith prepared from 25% wt monomer concentration had larger bead size than the monolith which was prepared from 50% wt monomer concentration. Similarly, the large void fraction was observed in the monolith with 25% wt monomer concentration while the monolith with 50% wt monomer concentration had smaller void fraction. It was clear from the SEM micrographs that the effect of monomer concentration on the bead size of monolith was significant. It could be conclude that, increasing the concentration of the monomer mixture led to smaller beads and less void fraction. Because high amount of divinyl monomer led to the formation of more crosslink polymers and phase separation. Although, this crosslink affected the swelling with the monomers, they remained relatively small in size. The pre-globules could still capture the nuclei generated during the polymerization process, but true coalescence did not occur. Since the final macroporous structure consisted of smaller globules, it also had smaller voids. Thus, this approach is useful for the preparation of monoliths with very large surface areas [34].

The morphology of the monoliths is also related with the types of the porogenic solvent as well as the concentration of monomer mixture. Yu et al. carefully studied the influence of methanol as porogenic solvent in GMA-EDMA polymerization and showed that the content of methanol could be tuned to achieve the desired porous properties of this monolith [35]. Peter et al. presented that hydrophilic porogenic solvent could be an alternative to control the porous property [35]. 1-deconol-cyclohexanol porogenic solvent induces the formation of small bead size while methanol promotes the formation of large bead size [35]. However, in this study, the mixture of methanol and ethanol was chosen as porogenic solvent because they are general chemicals commonly found in all laboratories. Other chemicals, such as dodecanol or cyclohexanol, are not widely available. Moreover, the requirement of large surface area or a small pore always is limited due to high back pressure.

It was observed that, by increasing the polymerization time, the bead size of the monolith decreased in both of 25 and 50 % wt monomer concentration. Therefore, the effect of polymerization time will be discussed in the next section.

4.1.2 Effect of Polymerization Time

The polymerization time is another parameter, which affects the morphology of the monolith. The monoliths were prepared by 25 and 50 % wt monomer in porogenic solvent that were polymerized at various time (10, 20, and 30 minutes) in order to study the effect of the polymerization time. The structures of the monolith's macropores were analyzed from SEM micrographs using Scion Image analysis and the results are shown in Table 4.1. We observed a significant effect of polymerization time on the morphology of monolith.

The monolith with 25% wt monomer concentration polymerized for 10 min had average bead size of 2.1 μn and 0.6 in void fraction which were larger bead size and void fraction when compared the monolith with 25% wt monomer concentration polymerized for 20 and 30 minutes. Similarly, the monoliths concentration at 50% wt prepared by UV exposure for 10, 20, and 30 minutes had the bead sizes decreased from 0.250 to 0.224 and to 1.93 μm, respectively. Therefore, it could concluded that increasing polymerization time could produce monolith with smaller bead size and smaller number of interconnected voids forming the channels for liquid flow. The decrease in bead size was resulted from an increase in crosslink density monomer in polymers as photoinitiation is prolonged as a direct consequence of increasing polymerization yield [33].

The polymerization time affects the kinetics of polymerization, which could be explained in terms of the nucleation rate or the formation of the pore. The polymerization started with the decomposition of the initiator to form a free radical. The polymer chain grew in solution as soon as possible before polymer chain precipitated as nuclei. The nuclei became swollen with the monomers and grew to micro-globules to a point where they crosslink between one another [36]. The longer polymerization time led to the formation of a larger number of free radicals by decomposition of the initiator. As a result, a larger number of pores and globules were formed. Due to the volume of monomers used was the same for each polymerization while the exposure time was longer, the array of interconnected globules was compensated by their smaller size [34]. Consequently, increasing the number of globules and microspheres necessarily decreased their size so that smaller voids or pores between them appeared in the final copolymer.

4.2 Modification the Monolith's Surface and Characterization

In this section, the (GMA-EDMA) monoliths with various compositions from previous section were modified by using sodium-hydrogen sulfide (NaSH) as a reagent in the nucleophilic substitution reaction. The poly (GMA-EDMA) monolith has the reactive epoxy groups on the surface that easily allow for the ring-opening under basic condition and transforms to thiol-groups according to the reaction in Figure 3.2.

To ensure that there were the thiol-groups on the monolithic surface after surface modification, quantitative determination of the generated thiol-groups was necessary. To determine the concentration of thiol group on the (GMA-EDMA) monolith, 2'2-dipyridyl disulfide (DPDS) was used as a reagent in the disulfide exchanger reaction following Figure 3.3. This reaction produces the mixed disulfide and equimolar amounts of pyridine-2-thiol being in equilibrium with the tautomeric form of pyridine-2-thione. The pyridine-2-thione concentration is proportional to the amount of thiol groups on the monolith surface. To determine the pyridine-2 -thione concentration,

DPDS solution was filled into the modified monolith in capillary and the reaction was allowed to complete within 1 hour. In the present study, pyridine 2 thione could be determined specifically at 440 nm by a photometric measurement. A calibration curve was constructed by using 2-mercaptoethanol as a standard. The calibration curve was shown in Appendix A.

Table 4.2 The amount of thiol groups generated on the monolith surface.

Monolith concentration	Polymerization Time (min)	Amount of thiol group (µmol)	% epoxy group being modifified
25%	10	0.034	4.46
	20	0.043	5.64
	30	0.060	7.88
50%	10	0.071	9.32
	20	0.099	13.00
	30	0.119	15.63

Assuming a complete incorporation of GMA into the polymer should contain a total of about 0.76 µmol epoxy groups (corresponding to about 4.23 $mmolg^{-1}$ polymeric materials). The monolith was about 0.2 mg. The result indicated that as the monomer concentration increased, the number of thiol groups increased. Increasing the monomer concentration led to more reactive epoxide-groups on the monolith surface. Thus, the monolith with 50% monomer concentration contained more thiol groups than did the monolith with 25% monomer concentration. Higher surface area had more epoxide atoms to attach the thiol molecules, leading to higher number of thiol groups generated on the monolith surface. As shown in Preinerstorfe et al, higher surface had more coverage with pendent thiol groups [3].

However, the amount of the thiol groups were lower than the theoretical number of total epoxy groups in the polymeric material. It is believed that significant portion of epoxy groups was buried inside the polymer globules of the monolith skeleton and could not react. For example, Preinerstorfe, et al. reported that 17% of total epoxide of the monolithic substrate could be transformed to reactive thiol groups. They performed the optimization of the reaction conditions for the transformation of epoxy groups to terminal thiol groups. The effect of variables such as reaction time, pH, temperature, and concentration of hydrogen sulfide, on the resultant thiol groups were investigated. According to the bimolecular reaction mechanism, when the sodium hydrogen sulfide concentration was increased, it could enhance the kinetic of the epoxide ring opening with sulfide. However, at higher concentrations sodium hydrogen sulfide (more than 2 M of sodium hydrogen sulfide), it found no improvement because it was no longer soluble under weakly basic conditions [3].

4.3 FTIR Analysis

The reactions that occurred during the epoxide ring opening and the crosslinking were studied by Fourier transform infrared spectroscopy (FTIR). An infrared spectrum represents a fingerprint of a sample with absorption peaks which correspond to the frequencies of vibrations between the bonds of the atoms making up the material. Because each different material is a unique combination of atoms, no two compounds produce the exact same infrared spectrum. Therefore, infrared spectroscopy can result in a positive identification (qualitative analysis) of every different kind of material. In addition, the size of the peaks in the spectrum is a direct indication of the amount of material present.

Firstly, an FT-IR analysis was carried out on GMA-co-EDMA monolith to validate that the epoxy ring was generated on the monolith surface after the polymerization reaction. The infrared spectrum of the monolithic polymer is shown in Figures 4.11.

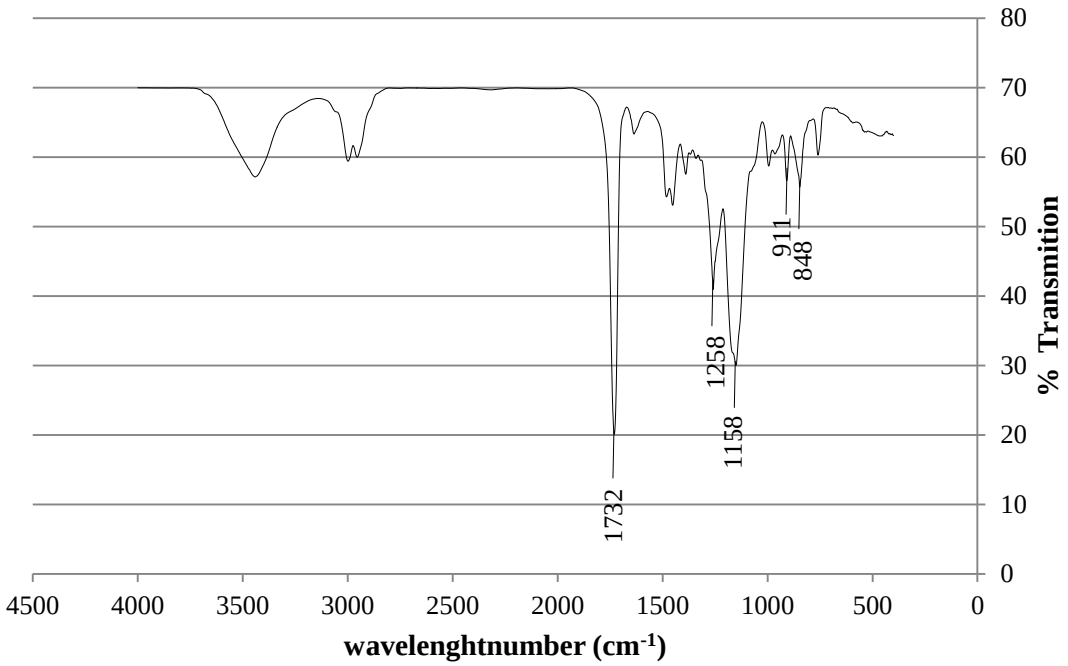

Figure 4.11 The infrared spectrum of GMA-co-EDMA monolith.

From Figure 4.11, the bands of the GMA-co-EDMA polymer was found at 848 cm^{-1}, around 911 cm^{-1} (epoxide ring vibration), 1258 cm^{-1} (d(C-O) epoxide) and 1158 cm^{-1} (d(C—O—C) crosslink). These peaks indicated the presence of epoxy groups. The broad band at 1732 cm^{-1} was attributed to the ester carbonyl stretching of both EDMA and GMA units. The functions and region of wavelength were referenced from Interpretation of Infrared Spectra by John Coates [48].

After the monolith modification with NaSH, the epoxide ring was opened and the thiol group was generated. The infrared spectrum of the modified monolith was different from the unmodified monolith due to the change via nucleophilic substitution. The infrared spectrum of the modified monolith was established as shown in Figure 4.12.

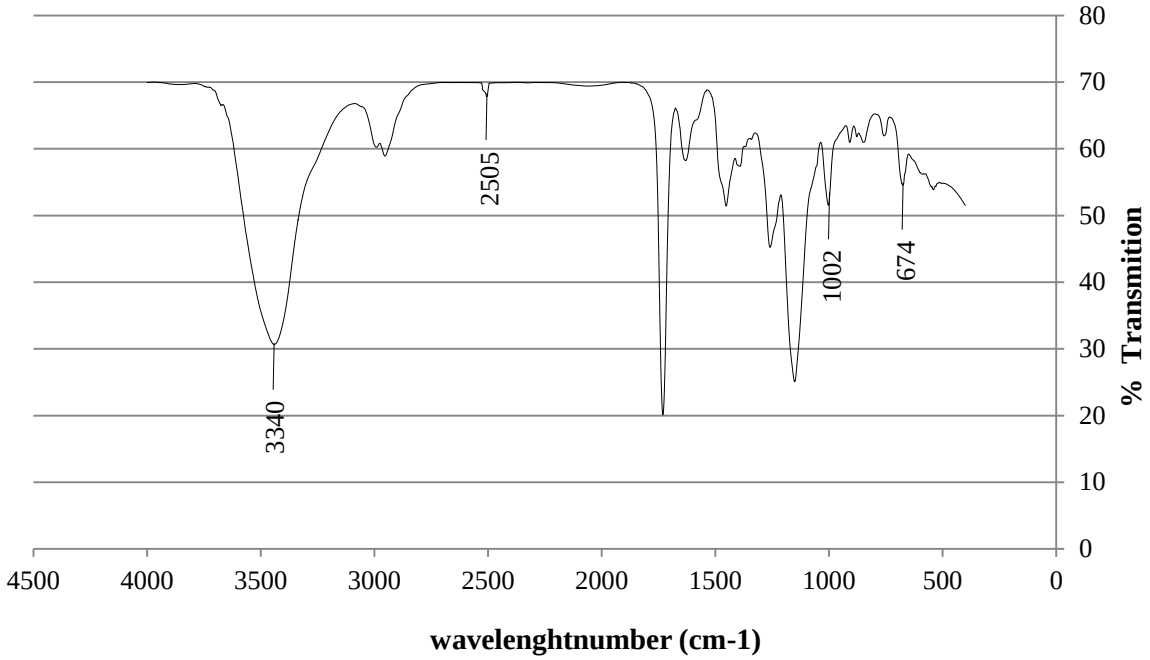

Figure 4.12 The infrared spectra of modified monolith.

When compare Figure 4.11 and 4.12, it was found that there were new peak appeared and some peaks disappeared. From these infrared spectrum, the bands of the modified monolith were found at 2505 cm^{-1}(d(S-H)) and at 674 (C-S stretch), indicating the presence of thiol group. The band at 3340 cm^{-1} is a characteristic of hydrogen bonded OH groups. Hydroxyl groups were formed in the basic-catalyzed epoxy ring opening reaction. Moreover, the existing of C-O component for the alcohol group was found at 1002 cm^{-1}. From these infrared spectrum, the peaks around 848 and 910 disappearred due to a decrease in the epoxide ring content after the neucleophilic substitution reaction with NaSH.

4.4 Stability of Cysteine

Cysteine was selected as a model thiol compound. It is used in the mobile phase to flow through the modified-monolith in glass capillary in order to form a disulfide bond with the modified-monolith. In this study, cysteine was detected by UV-spectrophotometer. Therefore, a wavelength scan of cysteine must be performed to obtain the specific wavelength which has the maximum UV-light absorbance value. The results are represented in forms of a graphical plot of the wavelength scan as shown in Figure 4.13.

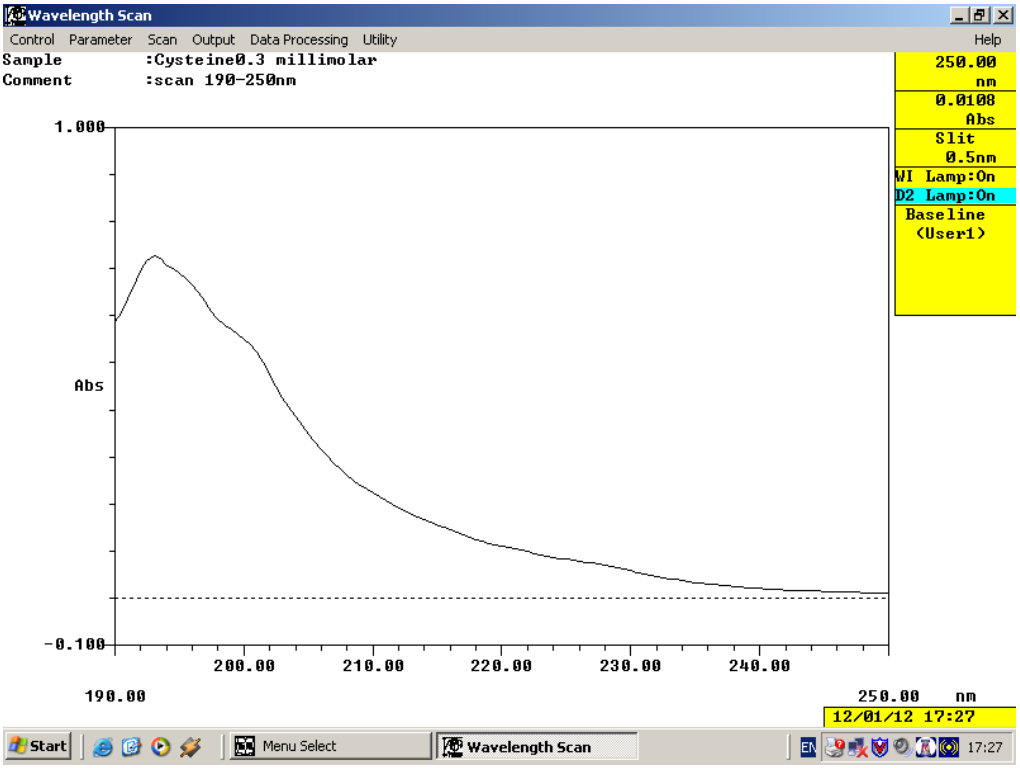

Figure 4.13 Wavelength scan of 0.3-millimolar cysteine in water**.**

It was found that a wavelength at 193.5 nm provided a maximum peak in the graph. It was chosen as a measured point.

4.5 Preconcentration of Cysteine

Sample preconcentration is a critical operation generally required for the determination of trace amounts of compounds of interest for which the concentration in the original solution exceeds the detection limits of the instrumentation.

The preconcentration consists of adsorption and desorption processes. When cysteine solution flowed through the pore of modified monolith, cysteine was adsorbed onto the surface of the porous monolith while the remaining sample flowed out. After that, stronger solvent was added to the channel to elute cysteine trapped in the pore. Low volume of solvent was used to elute cysteine, leading to an increase in the concentration of cysteine. The amount of cysteine adsorbed onto the modified monolith was calculated from a mass balance between inlet and outlet cysteine. The outlet concentration of cysteine could be measured using UV spectrophotometer at 193.5 nm. Then, the adsorption efficiency was evaluated based on the amount of cysteine at the inlet. In this study, the optimum inlet flow rate of cysteine was selected from Archiraya's study. The optimal inlet flow was 10 µl/min which provided the highest adsorption efficiency [6].

4.5.1 Adsorption efficiency of cysteine

In the study of the adsorption of cysteine, the modified monoliths as the stationary phase were prepared at different concentrations of monomer mixture and were used as an adsorbent like pack-bed polymer. 0.3 millimolar of cysteine was fed through the modified monoliths in the capillary tube using a syringe pump at the feed flow rate of 10 µl/min, while keeping the operation time constant at 90 minutes. The outlet of cysteine was collected in a vial to measure its absorbance and converted to the outlet concentration. Then, the amount of adsorbed cysteine was calculated from different amount of inlet and outlet cysteine. The formula for adsorption efficiency is expressed in the following equation.

$$\text{Adsorption Efficiency} = \frac{\text{Amount of cysteine adsorbed} \quad \text{X } 100}{\text{Amount of cysteine fed through the system}}$$

Table 4.3 Adsorption efficiency of modified monoliths at different concentration of monomer mixture and polymerization time using 0.3-millimolar-cysteine.

Monolith concentration	Polymerization time (min)	Amount of cysteine (µmol)			Efficiency (%)
		Inlet	Outlet	Adsorbed	
25%	10	0.27	0.205	0.065	24.3 ± 1.17
	20	0.27	0.175	0.095	35.1 ± 0.67
	30	0.27	0.160	0.110	40.7 ± 1.42
50%	10	0.27	0.166	0.104	38.7 ± 0.44
	20	0.27	0.118	0.152	56.2 ± 0.85
	30	0.27	0.112	0.158	58.3 ± 0.81

According to Table 4.3, the monolith with 50% monomer polymerized for 30 min had the highest adsorption efficiency due to a larger surface area. This large surface area allowed for a larger amount of liquid solution to be transferred or to be adsorbed within the capillary, resulting in a greater possibility of mass transfer. Consequently, the monolith with 50 wt% monomer polymerized for 30 min was an appropriate monolith for the preconcentration of cysteine solution. The adsorption efficiencies using the thiol-modified monolith were much higher than those of the EDMA-BuMA monoliths used in Achiraya's study. Cysteine was adsorbed onto EDMA-BuMA monolith via physical adsorption which was not as effective as chemical adsorption used in this study.

To confirm that the chemisorption was more effective than the physisorption, the adsorption efficiencies of the modified monolith were compared to those of the unmodified GMA-EDMA monolith, as shown in Table 4.4.

Table 4.4 Comparison of adsorption efficiency of 0.3 millimolar cysteine between monolith and modified-monolith**.**

Monolith concentration	Polymerization Time(min)	Adsorption efficiency (%)	
		GMA-EDMA monolith	Modified monolith
25%	10	16.7 ± 0.69	24.3 ± 1.17
	20	18.9 ± 0.29	35.1 ± 0.67
	30	21.8 ± 0.76	40.7 ± 1.42
50%	10	30.8 ± 0.34	38.7 ± 0.44
	20	33.5 ± 1.78	56.2 ± 0.85
	30	36.2 ± 2.05	58.3 ± 0.81

As shown in Table 4.4, the modified monoliths provided higher adsorption efficiencies because the adsorption of cysteine through the unmodified GMA-EDMA monolith was the hydrophobic adsorption. The interaction force between adsorbent and adsorbant was weak. In contrast, the modified monolith had reactive thiol groups that could form a disulfide bond with cysteine. This adsorption type is called chemical adsorption. Therefore, it was concluded that physical adsorption alone was not sufficient. Chemical adsorption was then suggested.

4.5.2 Inlet Concentration of Cysteine

This section focused on studying the effect of the inlet concentration of cysteine in deionized water on the adsorption efficiency. Cysteine was dissolved in deionized water at various concentrations between 0.05 – 1 millimolar. The inlet flow rate of cysteine was kept constant at 10 µl/min for 90 minutes, similar to the previous study. The outlet cysteine after adsorption process was collected and determined the amount of cysteine outlet by UV-spectrophotometer. Therefore, the accumulated cysteine in the monoliths was calculated by performing a mass balance, similar to the previous section. The result of the adsorption efficiency at different inlet concentrations is presented in Table 4.5.

Table 4.5 Adsorption efficiency of the microchannel with the feed flow rate of 10 µl/min at various concentrations of cysteine.

Inlet concentration (millimolar)	Amount of cysteine (µmol)			Adsorption Efficiency (%)
	inlet	outlet	Absorbed	
0.05	0.045	0.028 ± 0.001	0.017 ± 0.001	37.03 ± 0.99
0.1	0.09	0.049 ± 0.001	0.040 ± 0.001	44.57 ± 1.14
0.2	0.18	0.085 ± 0.001	0.095 ± 0.001	52.59 ± 0.20
0.3	0.27	0.112 ± 0.001	0.156 ± 0.001	58.37 ± 0.41
0.5	0.45	0.224 ± 0.005	0.226 ± 0.005	50.27 ± 1.10
0.7	0.63	0.339 ± 0.006	0.290 ± 0.006	46.08 ± 0.88
1	0.90	0.505 ± 0.017	0.395 ± 0.017	43.85 ± 1.91

According to Table 4.5, it was found that an increase in the inlet concentration of cysteine led to an increase in the amount of cysteine adsorbed on the monolith surface, leading to a decrease in the outlet concentration of cysteine. Higher concentration contained a large amount of cysteine fed through the microchannel and more available cysteine to be adsorbed to the surface of the monolith. Therefore, the liquid sample, in which the concentration equaled to 1 millimolar provided the largest amount of cysteine accumulated. However, for the adsorption efficiency, the maximal adsorption efficiency (58.37%) was obtained when the sample consisted of 0.3 milimolar of cysteine. The adsorption efficiency increased as the concentration of cysteine raised from 0.05 - 0.3 millimolar. An increase in the adsorption efficiency at this concentration range was a result of an increase in the available amount of cysteine. In contrast, an increase in cysteine's concentration from 0.3 to 1 millimolar resulted in a decrease in the adsorption efficiency from 58.37 to 43.85 %. The higher concentration of inlet cysteine gave rise to a saturation of monolith so that adsorption efficiency decreased.

Compared with Archiraya's study, the maximum adsorption efficiency in her study at the best condition was approximately 35 % while the maximum value of our study was around 58 %. This was resulted from the differences in the type of monomer and the structure of the monoliths, and pologenic solvent. In the Archiraya's experiment, cysteine was adsorbed on the monolith via physical adsorption which was a weak bond while in this preconcentration study, cysteine was adsorbed on the monolith surface via chemical adsorption in the form of a disulfide bond which was a stronger bond. Consequently, cysteine could adsorb on the monolith surface very well. Therefore, 0.3 millimolar cysteine was chosen for the preconcentration study in the next section.

4.5.3 FTIR Analysis

Once cystiene in the samples flowed through the modified monolith, cysteine molecules adsorbed onto the monolith surface via chemical adsorption. The thiol group on the modified monolith reacted with the thiol group of cysteine to form a disulfide bond. The reaction that occured during disulfide formation was studied by Fourier transform infrared spectroscopy (FTIR). The FT-IR spectrum of the modified monolith after cysteine was adsorbed is shown in Figures 4.14

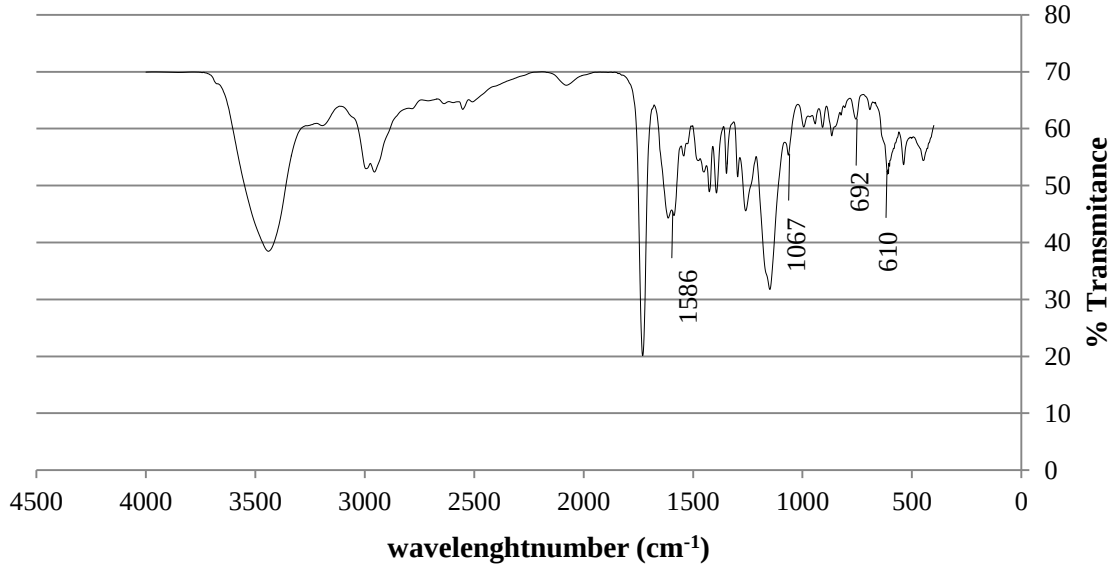

Figure 4.14 The infrared spectra of adsorbed cysteine on modified monolith.

The literature review gives characteristic peaks assigned to cystine in the finger print region at 620-600, 705–570 and 1650–1590 cm^{-1} attributed to S–S, C–S stretching and primary amine (N-H), respectively [48]. The peaks in the modified monolith after the adsorption of cysteine are present at 610, 692 and 1586 cm^{-1}. For R-COOH, the C-O-H bending was assigned at 1067 cm^{-1} [49]. In addition, the peak at 2505 cm^{-1} of (S-H) group was smaller than that of the modified monolith without adsorption because, after the adsorption, some of SH groups were converted to S-S, as a resulting of the binding between cysteine and GMA. It should be pointed out that FT-IR spectra of the cysteine and cysteine adsorbed on modified monolith are very similar, indicating the presence of cysteine on the surface of the monolith.

4.5.4 Elution of cysteine adsorbed on monolith

To preconcentrate cysteine, TCEP, as a reducing agent was added to the monolith in the capillary tube to break up the disulfide bonds between cysteine and the thiol groups on the monolith. Adsorbed cysteine would be extracted from the monolith. In order to increase the concentration of cysteine, lower volume of eluent was used. Therefore, the elution volume in this study was kept constant at 10 µL. The elution rate was varied from 3, 5, and 10 µl/hr. The elution time was varied depending on the elution rate to control the volume to be constant at 10 µL. After cysteine was extracted from the monolith, the outlet concentration of cysteine was calculated by constructing another

calibration curve of cysteine in TCEP solution. The elution efficiency and fold increase were also calculated from the following equations.

$$\text{Elution efficiency} = \frac{\text{Amount of cysteine eluted}}{\text{Amount of cysteine adsorbed on the monolith}} X100$$

$$\text{Fold increase} = \frac{\text{Outlet concentration of eluent}}{\text{Inlet concentration of fed sample}}$$

Table 4.6 The concentration and fold increase of cysteine after the preconcentration step at various elution rates.

Elution Rate (µl/hr)	Time (min)	Volume (µl)	Fold increase	Amount of cysteine (µmol)		Elution efficiency (%)
				Adsorbed	Eluted	
3	200	10	18.45 ± 1.56	0.153 ± 0.006	0.055 ± 0.004	36.06 ± 3.05
5	120	10	11.66 ± 0.62	0.166 ± 0.004	0.035 ± 0.002	21.07 ± 1.11
10	60	10	8.09 ± 0.73	0.158 ± 0.005	0.024 ± 0.002	15.36 ± 1.38

According to Table 4.6, a decrease in elution rate from 10 to 5 to 3µl/hr resulted in increasing cysteine concentration and a greater amount of cysteine being eluted, leading to better elution efficiency. The higher elution rate has relatively less elution time. Thus, it could imply that the elution rate at at 10 µl/hr yielded insufficient elution time, resulting in a lower fold increase in cysteine concentration. The best elution rate in this study is 3µl/hr, giving 18.45 fold increase in cysteine concentration, approximately twice as much as in Achiraya's study. It is possible that a flow rate lower than 3 µl/hr would give a more fold increase in cysteine concentration. However, longer elution time would be expected. The previous study has shown that the flowrate significantly affected the elution process. For example, 337 time enhancement of Coumarine519 concentration was achieved at flowrate of 3µl/min, while a much higher enhancement of 1650 times was obtained at a flowrate of 115 nL/min [26]. A low elution rate but prolonged elution time, e.g. elution at 1 µl/hr for 10 hours, is not practical for real applications. Therefore, we believe that 3 µl/hr is an optimum elution rate for cysteine preconcentration.

4.5.5 Regeneration of monolith

In addition, the monolith can be regenerated by a removal of cysteine residues, which reconstitutes the reactive sulfhydryl surface by using TCEP as reduction agent. As shown in Table 4.6, in the first reduction, the amount of eluted cysteine was relatively low while there still had a large amount of cysteine adsorbed on the monolith surface. The repetition of reduction reactions was investigated. Repeating TCEP flushing was necessary to test the reusability of the monolith concentrator which could be repeatedly

used for other experiments. Therefore, the use of a second or even a third reduction was necessary to achieve complete elution.

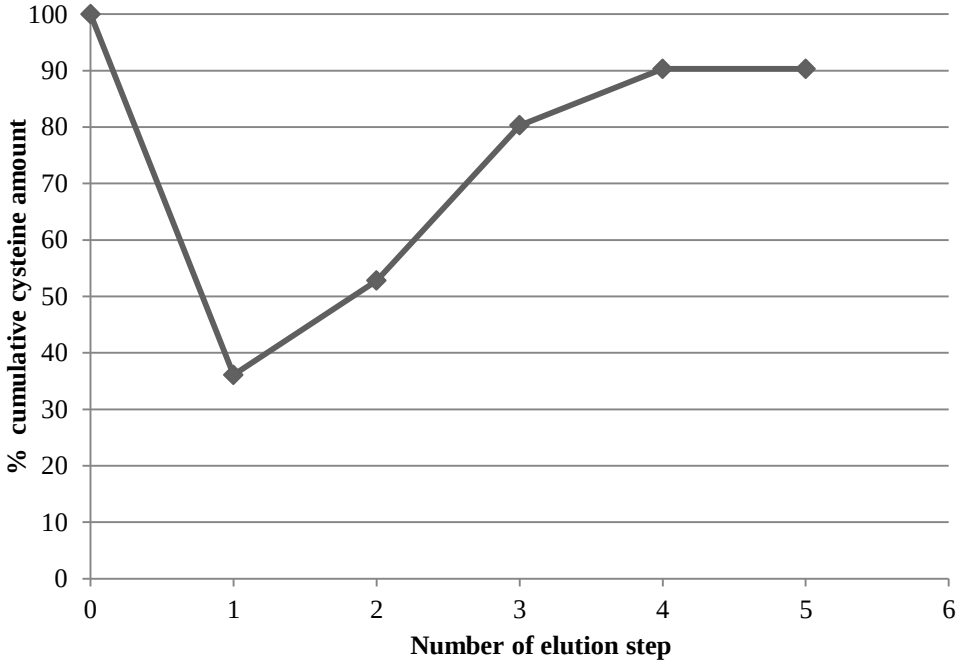

Figure 4.15 Cumulative of cysteine in elution steps.

In each elution step, 10 µl of TCEP solution was injected to the monolith in the capillary tube at a flow rate of 3µl/hr. About 36.1% of the original thiol groups could be regenerated after the first treatment. After flushing the capillary the second time with TCEP, about 60% of the thiol groups could be regenerated. It shows that more than 50% of cysteine could be eluted in the second time. In the other words, it had more than 50% of reactive sulfhydryl could be regenerated. However, to complete the elution of cysteine, a large number of reduction reactions were required. From the Figure 4.10, the elution procedure was consisted of 5 steps in order to completely elute cysteine which was adsorbed on the monolith surface. Therefore, reusing of monolith was not suggested because removing all cysteine adsorbed on the monolith surface required 5 step elution with TCEP which was a time-consuming process. Compared to Preinerstorfer et al. study, 67% of the original thiol groups could be regenerated after the first treatment. After flushing the capillary for the third time the reduction was completed [3]. The volume of TCEP in their study was 50 µl per each elution step which was higher than the elution volume in this study. Resulting from more volume of elution solution, it was contained more amount of TCEP so that % of disulfide removal was higher.

Table 4.7 The fold increase and %recovery of cysteine after elution steps.

Number of elution steps	1	2	3	4	5
Cysteine adsorbed	0.153	0.098	0.047	0.010	0.002
Cysteine desorbed	0.055	0.051	0.037	0.008	0.000
% elution efficiency	36.1	52.0	80.1	89.0	89.0
Fold increase	18.45	17.86	16.04	12.71	10.24
%recovery	36.1	69.77	93.99	99.4	100

From Table 4.7, resulting from higher the number of elution steps, the cumulative amount of cysteine was higher due to large volume of TCEP solution, but the fold increase was decreased. The cysteine was fully recovered (100%) after 5 elution steps. Cong Yu. and coworker reported that the elution of Courmarin 519 from ion-exchanger concentrators by using sodium salicylate solution at a reduction flow rate of 1 µL/min was not complete in the first elution step. The second elution step contained 48% Courmarin 519 of first elution [26]. In contrast, elution with sodium salicylate at reduction flowrate of 203 nL/min almost completely eluted Courmarin 519. Therefore, the results in this project were consistent with the experiment from Cong Yu *et al.* that the lower elution rate yielded higher elution efficiency.

CHAPTER 5 CONCLUSION AND RECOMMENDATIONS

5.1 Conclusion

The monolithic polymer was successful synthesized inside a glass capillary by UV polymerization. Glycidyl methacrylate (GMA) and ethylene dimethacrylate (EDMA) were selected as monomers, while porogenic solvent consisted of methanol and ethanol and DAP was used as an initiator. The length of monolith was about 10 mm to avoid the back pressure and the low flow resistance was required when liquid flow through. The monolithic polymer was characterized by varying the monomer concentrations between 12.5, 25, and 50 wt%, and the polymerization durations from 10, to 20, and 30 min. The higher monomer concentration resulted in smaller bead size and less void fraction. Because of high amount of divinyl monomer led to formation of more crosslink polymers and phase separation. A large number of smaller micropores in the monolith and the interconnected void filled by later formed polymer balls resulted in larger surface area. Similarly, longer polymerization time resulted in smaller bead size and less void fraction. The aim of this study is the preconcentration of cysteine by chemisorption on surface of monolith polymer. Therefore, the adsorbed surface area was an important factor that affected to adsorption mechanism. A monolith with large surface area was preferred for better adsorption. Consequently, the monoliths prepared with 50 wt% monomers and polymerized for 30 min were selected for further study in preconcentration of cysteine.

In the second step, the monolithic polymer was modified by transformation of epoxide groups of the polymer streaming from GMA monomer by nucleophilic substition reaction with sodium hydrogen sulfide. The amount of reactive thiol groups generated on monolith surface could be determined in a disulfide-exchanger reaction using 2,2’ dipyridyl disulfide. It possible that the thiol groups on monolith surface could for a bond with cysteine via a disulfide bond. Therefore, the modified monolith polymer was used as stationary phase for cysteine preconcentration.

Cysteine was prepared in deionization water as mobile phase then, injected through the modified monolith surface using a syringe pump at 10 µl/min. The chemisorptions would occur. The inlet concentrations of cysteine were varied between 0.05 - 1 millimolar to verify the condition that gives the highest adsorption efficiency. The maximum adsorption efficiency was found to be 58.37% when the sample consisting of 0.3 millimolar of cysteine. Finally the amount of cysteine adsorbed on the modified monolith was eluted by using TCEP 50 molar in excess. The best elution rate in the

present study is 3µl/hr, giving a 18.45 fold increase in cysteine concentration. It is believed that the elution efficiency could be further improved if the elution time was prolonged with a lower elution rate. In addition, 5 elution steps were required to remove all cysteine adsorbed on monolith surface and the thiol groups on the monolith were regenerated. For the highest fold increase, only one elution step with TCEP is required.

5.2 Recommendation

- The complete polymerization of the monolithic polymer should be investigated by prolonging the polymerization time e.g. 40 min. Furthermore, to acquire more accurate results, the monomer concentration and polymerization time should be studied in more details.

- To avoid the cracking of the polymerized monolith during cutting process before visualizing the morphology of monoliths by SEM, the laser cut could provide a precise edge cut of the monoloth. Furthermore, this would ensure that the voids of monolith revealed SEM micrograph were not caused by the cracking during cutting process.

- There was a gap between the monolith and the capillary wall thus the capillary wall was pre-treatment before monolith synthesis.

-Since a UV spectrophotometer has low sensitivity and limited the detection of cysteine concentration at 0.1 millimolar, a more sensitive analytical instrument, such as, HPLC should be used instead of a spectrophotometer for an analysis of a sample containing a trace amount of an interested compound.

REFERECES

[1] Keith E. Herold and Avraham Rasooly, 2009, **Fabrication and Microfluidics**, Caister Academic Press**,** UK, pp.1-409

[2] Bhupinder Singh Sekhon and Seema Kamboj, 2010, "Microfluidics Technology for Drug Discovery and Development", **International Journal of PharmTech Research**,Vol.2, pp. 804-809.

[3] Beatrix Preinerstorfer, Wolfgang Bicker, Wolfgang Lindner, Michael Lämmerhofer,2004, "Development of reactive thiol-modified monolithic capillaries and in-column surface functionalization by radical addition of a chromatographic ligand for capillary ectrochromatography", **Chromatography A**, Vol. 1044 pp. 187–199.

[4] Siobhan E. Moriary, Jheel H. Shah, Michael Lynn, Shunai Jiang, Kyle Openo Dean P. Jones and Paul Sternberg, JR., 2003, "Oxidation of glutathione and cysteine in human plasma associated with smoking", **Free Radical Biology & Medicine**, Vol. 35, No. 12, pp. 1582–1588.

[5] Wei Wang, Liang Zhaoa, Fang Zhoua, Jun-Jie Zhua, Jian-Rong Zhang, 2007, "Electroosmotic flow-switchable poly(dimethylsiloxane) microfluidic channel modified with cysteine based on gold nanoparticles", **Talanta**, Vol. 73, pp. 534–539.

[6] Archiraya, 2007, **Delvelopment of a microfluidic sample preconcentration system for Cysteine using BuMA-EDMA monolith**, Master of Engineering Thesis, Chemical Engineering, Faculty of Engineering, King Mongkut's University of Technology Thonburi, pp. 1-89.

[7] Wikipedia, 2011, **Polydimethylsiloxane** [Online], Available: http://en.wikipedia.org/wiki/Polydimethylsiloxane, [2011, April 8].

[8] Chow, W.Y., Lei, K.F., Shi, G., Li1, W.J. and Huang, Q., 2006, "Microfluidic Channel Fabrication by PDMS-Interface Bonding", **Institute Of Physics Publishing**, Vol. 15, pp. 112-116.

[9] Waldner, Jean-Baptiste, 2008, **Nanocomputers and Swarm Intelligence**,John Wiley & Sons, London, pp. 92–93.

[10] H.B. Lima, Donghoon Kima, Taeyoon Jung, R.S. Houk, Yangsun Kimc., 2005, "A radiofrequency plasma in a polydimethylsiloxane (PDMS) microchip", **Analytica Chimica Acta**, Vol. 545, pp.119–121.

[11] Wikipedia, 20011, **Soft lithilography** [Online], Available: http://en.wikipedia.org/wiki/Soft_lithography, [2011, April 9].

[12] Younan Xia and George M., 1998, "SOFT LITHOGRAPHY", **Mater Science**, Vol. 28, pp. 84-153.

[13] Biomem Resource Center, 2007, **Procedure for Photolithography** [Online], Available: http://www.biomemsrc.org/biomems/documents/photolithography.pdf, [2011, May 1].

[14] Junjie Ou, Tomasz Glawdel,b Carolyn L. Ren and Janusz Pawliszyn., 2008, "Fabrication of a hybrid PDMS/SU-8/quartz microfluidic chip for enhancing UV absorption whole-channel imaging detection sensitivity and application for isoelectric focusing of proteins", **Lab on a Chip**, Vol.56. pp 99-106.

[15] Shantanu Bhattacharya, Arindom Datta, Jordan M. Berg, and Shubhra Gangopadhyay., 2005, "Studies on Surface Wettability of Poly(Dimethyl) Siloxane (PDMS) and Glass Under Oxygen-Plasma Treatment and Correlation With Bond Strength", **Microelectromechanical system**, Vol.14, No. 3.

[16] James Friend,Leslie Yeo, 2010, "Fabrication of microfluidic molds", **Biomicrofluid**, Vol. 4, pp. 256-260.

[17] Massachusetts Institute of Technology, **Material Property Database** [Online], Available: http://www.mit.edu/~6.777/matprops/pdms.htm, [2011, May 23].

[18] Bryan, A., Langowski and Uhrich, K.E., 2005, "Oxygen Plasma-Treatment Effects on Si Transfer", **Langmuir**, Vol. 21, pp. 6366-6372.

[19] Hui Taek Kim, Ok Chan Jeong., 2011, "PDMS surface modification using atmospheric pressure plasma", **Microelectronic Engineering**, Vol. 23, pp. 239-248.

[20] Dhananjay Bodas, Chantal Khan-Malek., 2006, "Formation of more stable hydrophilic surfaces of PDMS by plasma and chemical treatment", **Microelectronic Engineering**, Vol. 83, pp. 1277–1279.

[21] Shaofeng Xie, Robert W. Allington, Jean M.J. Fréchet,Frantisek Svec, **Porous Polymer Monoliths:An Alternative to Classical Beads**.

[22] Ruben Dario Arrua, Miriam Cristina Strumia and Cecilia Inés Alvarez Igarzabal., 2009, "Macroporous Monolithic Polymers: Preparation and Applications", **Material**, Vol. 2, pp. 2429-2466.

[23] Mariano Grasselli, Eduardo Smolko, Peter Hargittai, Agnes Safrany., 2001, "From micospherea to monoliths : Synthesis of porous supports with tailored properties by radiation polymerization", **Nuclear instrument and Method in Physics research**, Vol. 185, pp.254-261.

[24] M. Bedair, Z. El Rassi, 2005, "Affinity chromatography with monolithic capillary columns", **Journal of Chromatography A**, Vol. 1079, pp.236.

[25] X.L. Dong, J. Dong, J.J. Ou, Y. Zhu, H.F. Zou, "The covalently bonded cellulose tris (3,5-dimethylphenylcarbamate) on a silica monolithic capillary column for enantioseparation in capillary electrochromatography", **Electrophoresis**, Vol. 27, pp. 2518.

[26] Yu, C., Davey, M.H., Svec, F., and Fre´chet, J.M., 2001, "Monolithic Porous Polymer for On-chip Solid Phase Extraction and Preconcentration Prepared by Photoinitiated in Situ Polymerization within Microfluidic Device", **Journal of Anal. Chem**, Vol. 73, pp. 5088-5096.

[27] Song, S. and Singh, A.K., 2006, "On-chip Sample Preconcentration for Integrated Microfluidic Analysis", **Anal Bioanal Chem**, Vol. 384, pp. 41-43.

[28] Rohr, T., Yu, C., Davey, M.H., Svec F. and Fre´chet, J.M., 2001, "Porous Polymer Monoliths: Simple and Efficient Mixers Prepared by Direct Polymerization in the Channels of Microfluidic Chips", **Electrophoresis**, Vol. 22, pp. 3959-3967.

[29] Nagano, N., Ota, M. and Nishikawa, K., 1999, "Strong Hydrophobic Nature of Cysteine Residues in Proteins", **FEBS Letters**, Vol. 458, pp. 69-71.

[30] Wikipedia, 2011, **Cysteine** [Online], Available: http://en.wikipedia.org/wiki/Cysteine, [2011, May 28].

[31] Chow, W.Y., Lei, K.F., Shi, G., Li1, W.J. and Huang, Q., 2006, "Microfluidic Channel Fabrication by PDMS-Interface Bonding", **Institute Of Physics Publishing**, Vol. 15, pp. 112-116.

[32] Jir Urban and Pavel Jandera., 2008, "Polymethacrylate monolithic columns for capillary liquid chromatography", **Science**, pp. 2521 – 2540.

[33] Katarzyna Chudaa, Joanna Jasika, Julien Carlierb, Pierre Tabourierb, Christian Druonb, and Xavier Coquereta., 2005, "Characteristics and fluidic properties of porous monoliths prepared by radiation-induced polymerization for Lab-on-a-Chip applications", **Radiation Physics and Chemistry**, Vol. 75, pp. 26–33.

[34] Frantisek Sveca,b., 2010, "Porous polymer monoliths: Amazingly wide variety of techniques enabling their preparation", **Chromatography A**, Vol. 1217, pp.902–924.

[35] Karine Faure, Nathalie Delaunay 1, Guillaume Alloncle, St´ephane Cotte, and Jean-Louis Rocca., 2007, "Optimization of in-situ monolithic synthesis for immunopreconcentration in capillary", **Journal of chromatography**, Vol. 1149, pp. 145-150.

[36] Eoin Gillespie, B.Sc., 2009, "**The formation, modification and characterisation of monolithic ion exchangers for separation science**", City University School of Chemical Sciences.

[37] Separation process, 2012, **Physical and chemical adsorption** [Online], Available: http://separationprocesses.com/Adsorption/AD_Chp01b.htm, [2012, January 9].

[38] Chemistrylearning, 2012, **Adsorption** [Online], Available: http://www.chemistrylearning.com/adsorption/, [2012, January 9].

[39] Meng Tang, Xuejun Cao, Zuozhen Liu , Xingyan Wu, Dai Gance., 1999,"Synthesis of glycidyl methacrylate-based matrix and its application in affinity chromatography of urokinase", **Process Biochemistry**, Vol. 34, pp. 857–862.

[40] Paul A. Webb., 2003, " Introduction to chemical adsorption analytical techniques and their applications to catalysis", **MIC Technical Publication**.

[41] Wikipedia, 2012, **Adsorption** [Online], Available: http://en.wikipedia.org/wiki/Adsorption, [2012, January 8].

[42] Rajee Singh, George M., Whitesides., 1994, "Reagent for rapid reduction of native bonds in proteins", **Bioorganic chemistry**, Vol. 22, pp. 109-115.

[43] Camilla Viklund, Frantisek Svec, and Jean M. J. Fre´chet., 1996, "Monolithic, "Molded", Porous Materials with High Flow Characteristics for Separations, Catalysis, or Solid-Phase Chemistry: Control of Porous Properties during Polymerization", **Chem. Mater**, Vol. 8, pp. 744-750.

[44] Rajee Singh, George M., Whitesides., 1991, " A reagent for reduction of disulfide bonds in protein that reduces disulfide bonds faster than dose dithiothreitol", **Organic chemistry**, Vol. 56.

[45] M.C. Whittle, J.F.Stobaugh, O.S.Wong., 2000, "Hihg performance liquid chromotographi method for the determination of homocysteine in human plasma using a water-soluable phosphine reducing agent and flurogenic derivatization", **Bioanalytical research**, Vol. 52, pp. 78-82.

[46] Daniel J., Cline. Sarah E.,Redding, Stephen G.,Brohawn James N., Psathas Joel P.,colin Thorpe., 2004, "New water-soluable phosphine as reductants of peptide and protine disulfide bond", **Biochemistry**, Vol. 43, pp. 15195-15203.

[47] Themo Scientific, 2012, **TCEP-HCl** [Online], Available: http://www.piercenet.com/browse.cfm?fldID=02051012, [2012, January 5].

[48] Coates J., 2000, "Interpretation of Infrared Spectra, A Practical Approach", **Encyclopedia of Analytical Chemistry**, pp. 10815–10837.

[49] Grisset Faget O., Judith Felcman, Tiago Giannerini b, Claudio A. Tellez S.,2005, "Fourier-transform infrared and Raman spectra of cysteine dichloride cadmium(II) anion", **Organic chemistry**, Vol. 61, pp.2121–2129.

[50] G. Chwatko, E. Bald, 2000, "Determination of cysteine in human plasma by high-performance liquid chromatography and ultraviolet detection after pre-column derivatization with 2-chloro-1-methylpyridinium iodide", **Talanta**, Vol. 52 pp.509–515.

APPENDIX A

Standard Curve of Cysteine

Cysteine in solution was detected using UV spectrophotometer (U-3000) to examine its concentration. In a spectrophotometer, the concentration of the sample is determined as an absorbance based on the adsorption of the light. The absorbance of a sample is proportional to the thickness of the sample and the concentration of the absorbing substances in the sample. The absorption refers to the physical process of absorbing light, while absorbance refers to the mathematical quantity. However, any real instrument has a limited measure over which it can accurately measure absorbance. It is difficult to perform accurate measurement in very small absorbances that are very close to zero absorbance. The theoretical best accuracy for most instruments is in the range near 1 AU. The path length or concentration should be adjusted to achieve readings near this range.

Initially, the wave length scan by U-3000 spectroschopy shown in Figure A.1 was performed to investigate which wave length must be specified to determine the concentration of cysteine for the standard curve for the UV detection.

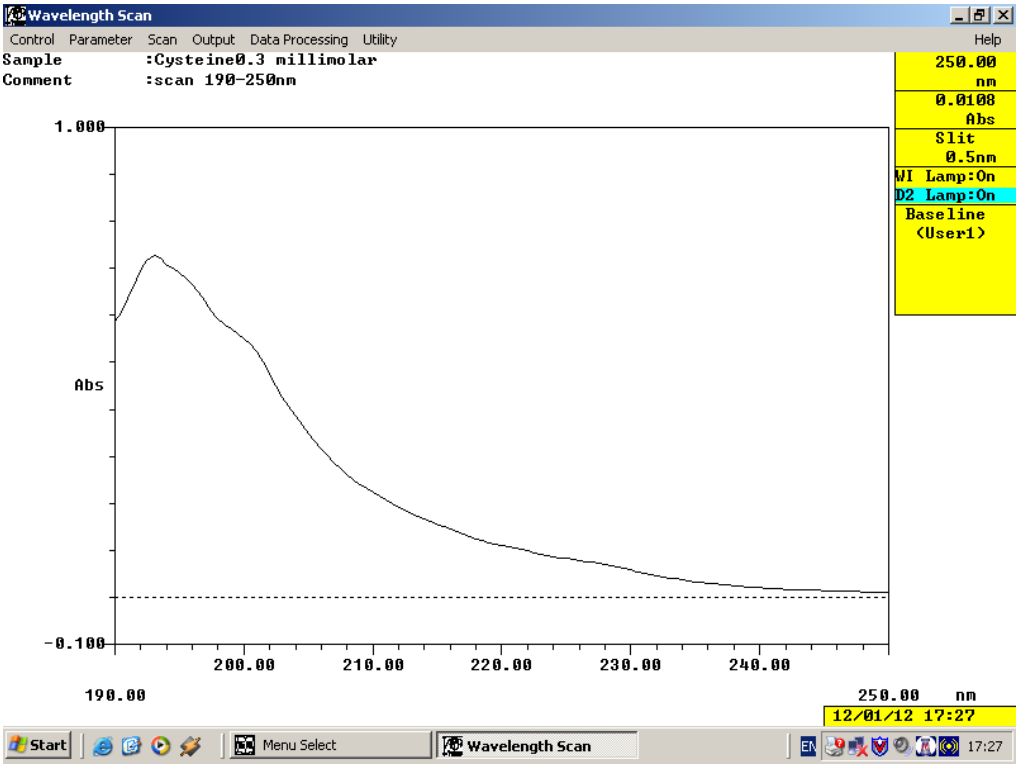

Figure A.1 Wavelength scan of 0.3-millimolar cysteine in water

It was found that the 193.5-nm wave length providing a maximum point or a peak in the scan was chosen as measured point. The standard curve of cysteine in TCEP was then performed to further verify the concentration of cysteine eluted by TCEP solution. The interesting cysteine concentration is in the range of 0.01-1 millimolar, If the concentration of cysteine in TCEP and water expressed in the further experiment exceeds these ranges, it is necessary to dilute the concentration to ensure it is measurable.

Table A.1 Absorbance data of cysteine in water measured at 193.5 nm.

Concentration (millimolar)	Absobance			Average
	#1	#2	#3	
0.05	0.1627	0.1565	0.1603	0.1598
0.1	0.3311	0.3259	0.3305	0.3291
0.15	0.4166	0.4197	0.4197	0.4179
0.2	0.5899	0.5829	0.5829	0.5864
0.25	0.6771	0.6783	0.6783	0.6781
0.3	0.8810	0.8699	0.8699	0.8737

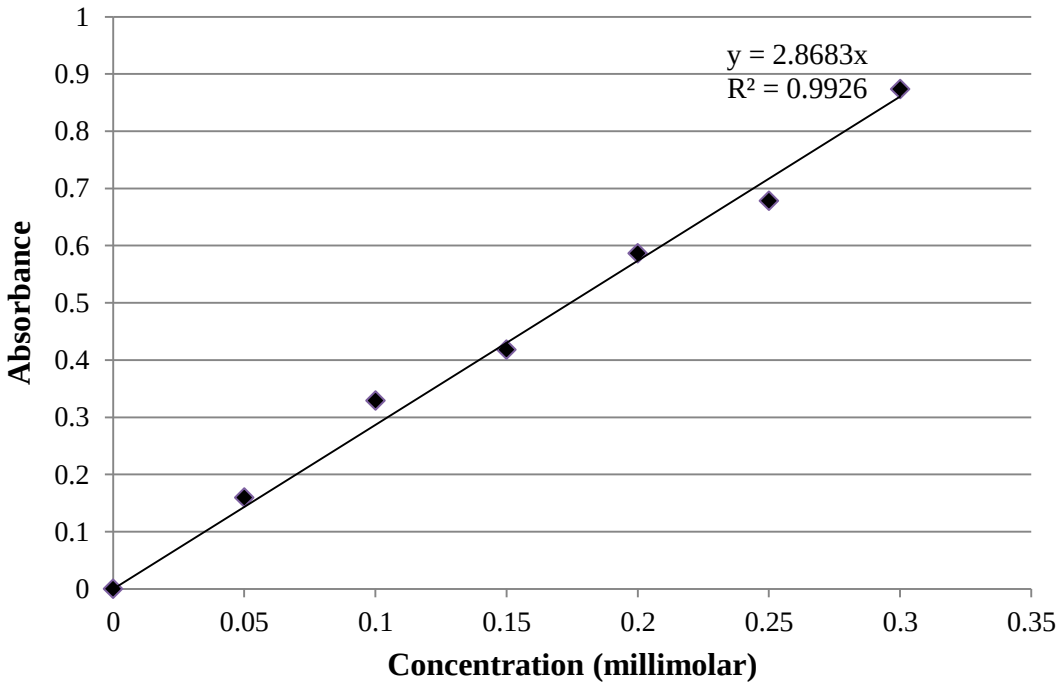

Figure A.2 Standard curve of cysteine in water

Table A.2 Absorbance data of cysteine in TCEP measured at 232.5 nm

Concentration (millimolar)	Absorbance			Average
	#1	#2	#3	
0	0.0006	0.0005	0.0001	0.0004
0.1	0.0693	0.0723	0.0722	0.071267
0.3	0.1454	0.1398	0.1465	0.1439
0.5	0.2212	0.2241	0.2189	0.2214
0.7	0.3106	0.3115	0.3102	0.310767
1	0.4761	0.4783	0.4812	0.478533

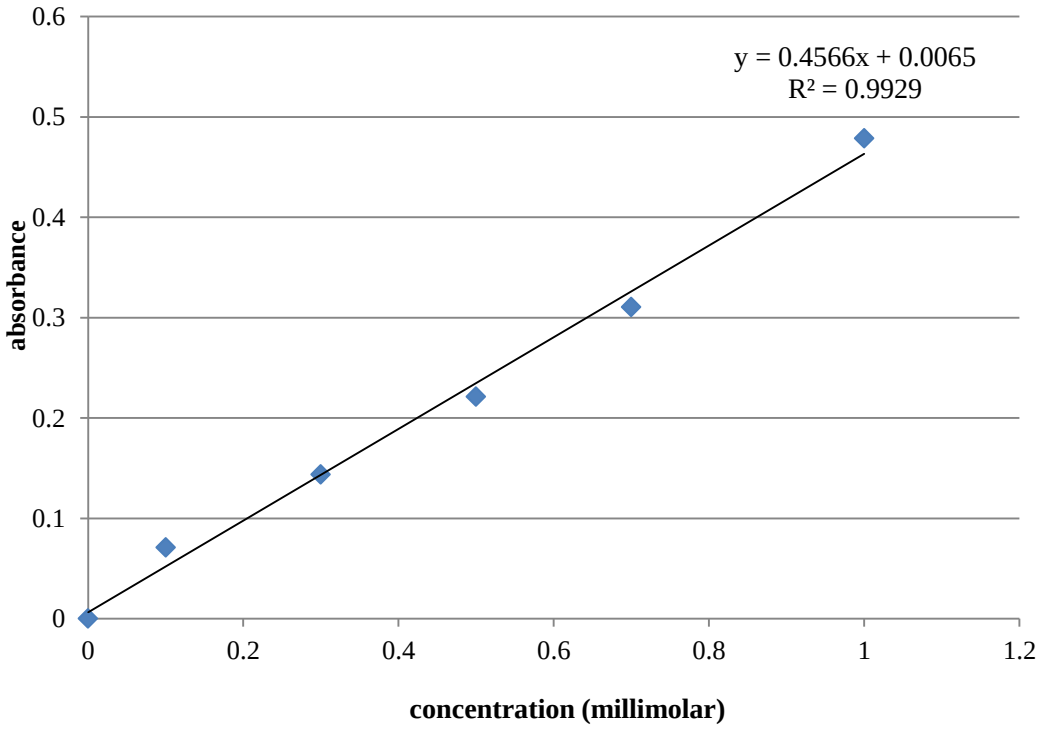

Figure A.3 Standard curve of cysteine in TCEP

APPENDIX B

Scion Image Analysis

In order to evaluate the bead sizes and void fraction between the beads, the image analysis was performed through SEM micrographs and Scion image analysis software.

B.1 Scion Image Analysis

Scion Image is a program for processing and analyzing images. It allows for better visualization and provides tools for the quantitative analysis of pictures. Scion Image Analysis can be used to measure area, mean, centroid, perimeter, etc. of user defined regions of interest. It also performs automated particle analysis and provides tools for measuring path lengths and angles. Spatial calibration is supported to provide real world area and length measurements. Density calibration can be done against radiation or optical density standards using user specified units. Results can be printed, exported to text files, or copied to the Clipboard. A tool palette supports editing of color and gray scale images, including the ability to draw lines, rectangles and text. It can flip, rotate, invert and scale selections. It supports multiple windows and 8 levels of magnification. All editing, filtering, and measurement functions operate at any level of magnification and are undoable.

B.1.1 Image Preparation

1.1 Open text file (*.txt) from SEM analysis in order to check the size of image in terms of pixels (1280×960) and real length of the sample recorded by SEM (e.g. 26.4 μm) as shown in Figure C.1

1.2 Divided the image size by the real length (e.g. $\frac{1280}{26.4} = 48.48484$) to calculate the pixels per micrometer for inputting in the scale setting in Scion Image

1.3 Convert the image file into TIFF format using Photoshop.

1.4 Start the Scion Image program.

1.5 When the program starts up, select the “Import” command in the “File” menu.

1.6 Select the desired image that their file extensions are in TIFF format (it is necessary to make sure that it is decompressed, since Scion Image cannot open compressed files.), and double click to open it.

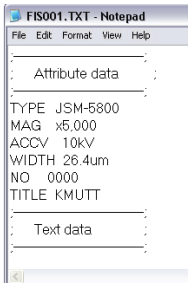

Figure B.1 Text file of details for SEM micrograph

B.1.2 Scale Setting

2.1 Select the "Set Scale" command in the "Analyze" menu. The pop-up menu for the scale setting will instantly appear as seen in Figure C.1, C.2.

2.2 Select micrometers in the "Unit" submenu to convert the unit in terms of micrometers.

2.3 Enter the calculated value pixels per micrometers (e.g. 48.4848) for Scale.

2.4 Click OK. Now distances show in the Info window in units of micrometers.

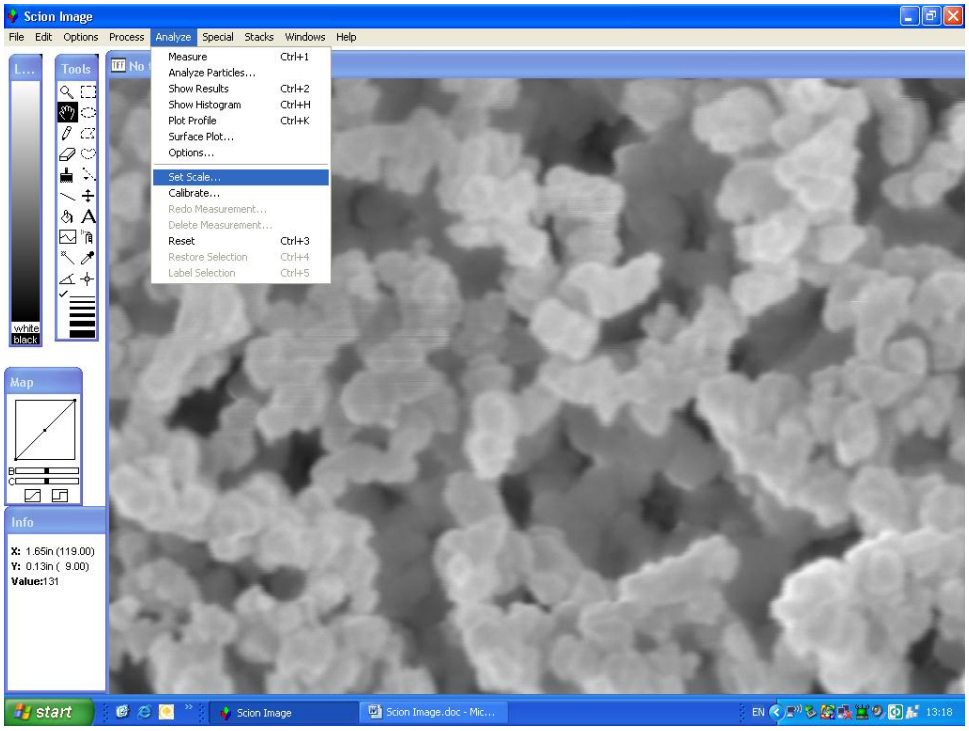

Figure B.2 An opened image in Scion Image Analysis for scale setting

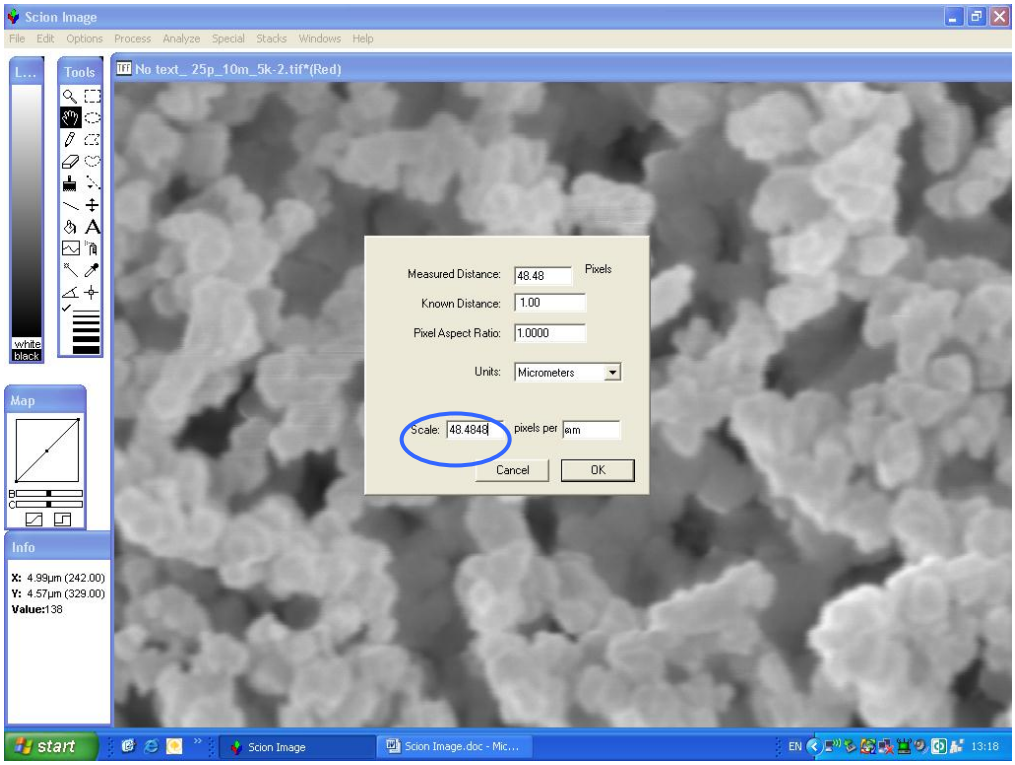

Figure B.3 Scale setting in Scion Image Analysis

b.1.3 Bead Size Calculation

3.1 Select the “Options” command in the “Analyze” menu.

3.2 Choose “Perimeter/Length” in the “Measurement Options” for the measurement of the bead size in micrometers shown in Figure C.4.

3.3 Considering at the image, select in the “Tools” window.

3.4 Drag over to the right side of the polymer bead in the image; select the item “Measure” command in the "Analyze" menu.

3.5 Repeat the measurement for each polymer bead (40 times).

3.6 Select the item “Show results” from the “Analyze” menu. The results are illustrated in forms of table as shown in Figure C.5

3.7 Use statistic information to calculate the average and standard deviation of polymer beads.

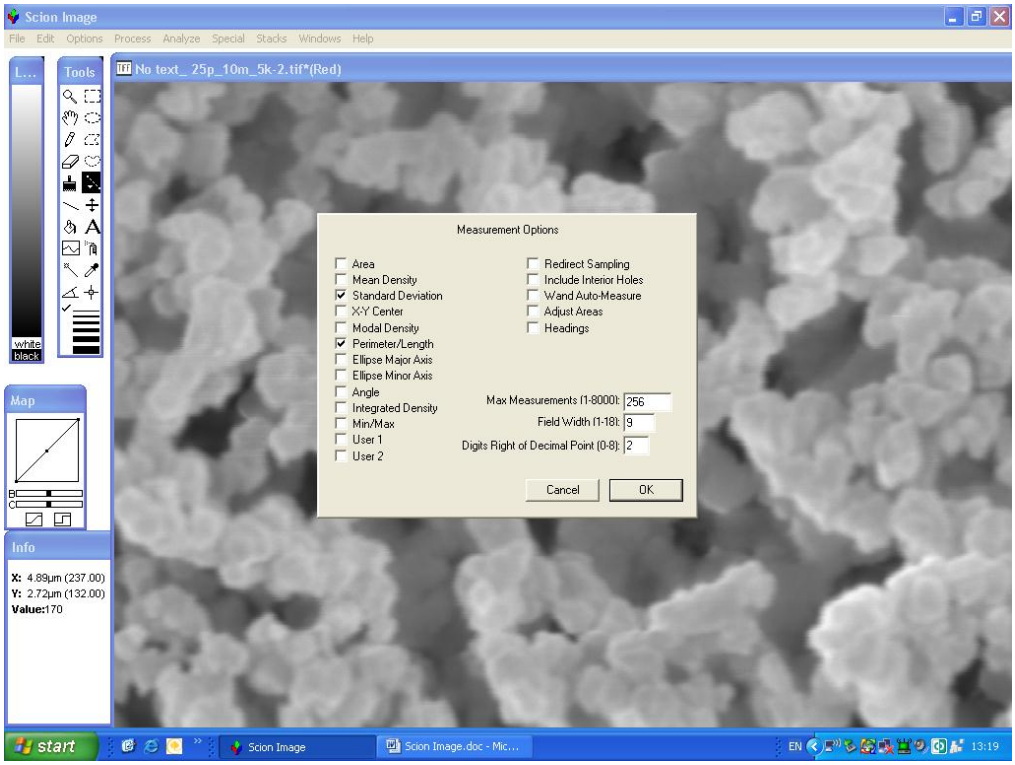

Figure B.4 The pop up window for setting length in the measurement options

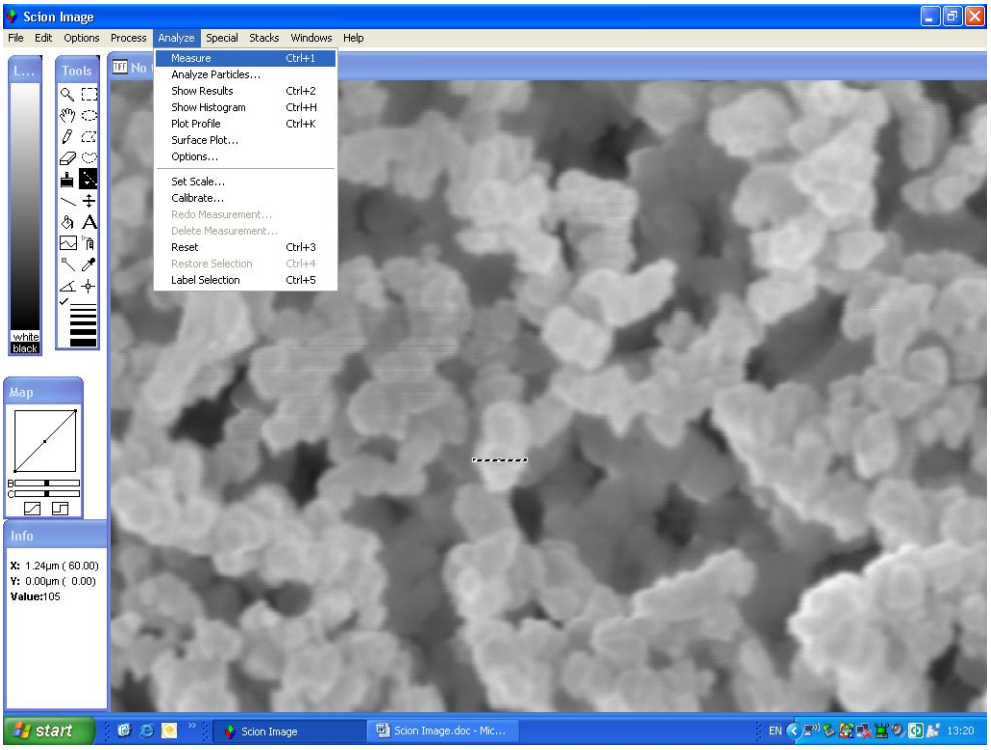

Figure B.5 The measured length each polymer bead

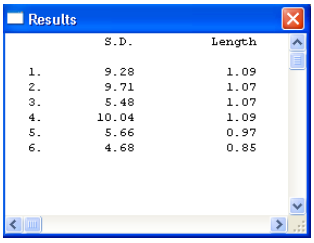

Figure B.6 The results in forms of Table expressed as pop-up window

B.1.4 Void Fraction Calculation

The void fraction is calculated from the ratio of void area to total are as shown in following equation:

$$\varepsilon = \frac{\varepsilon_v}{\varepsilon_t} \tag{C.1}$$

where ε is void fraction, ε_v is void area, and ε_t is total area

Both areas can be estimated using threshold function. Thresholding is used to segment an image into objects of interest and background on the bases of gray level. When thresholding is enabled, objects are displayed in black and background is white.

4.1 Select the “Options” command in the “Analyze” menu.

4.2 Choose “Area” in the “Measurement Options” shown in Figure C.7.

4.3 Select the item "Threshold" command in the "Options" menu. The threshold is automatically set based on an analysis of the histogram of the entire image. The image turns fully black and white as shown Figure C.8

4.4 To vary the threshold, use the LUT tool appearing on the left of the window and click and drag near the black and white boundary. (Generally, threshold value is set as the default value from the software)

4.5 Select the “Measure” command in the “Analyze” menu. In the Info window, it is expressed the area in square micrometers.

4.6 The area recorded is presented in the table by selecting "Show results" from the "Analyze" menu.

4.7 In order to calculate the total area, the picture is turned into black by adjust the threshold values to 1.0. (See Figure C.9)

4.8 Select the "Measure" command from the "Analyze" menu.

4.9 Record the total area on the results table.

4.10 Calculate void fraction by using the equation mentioned above.

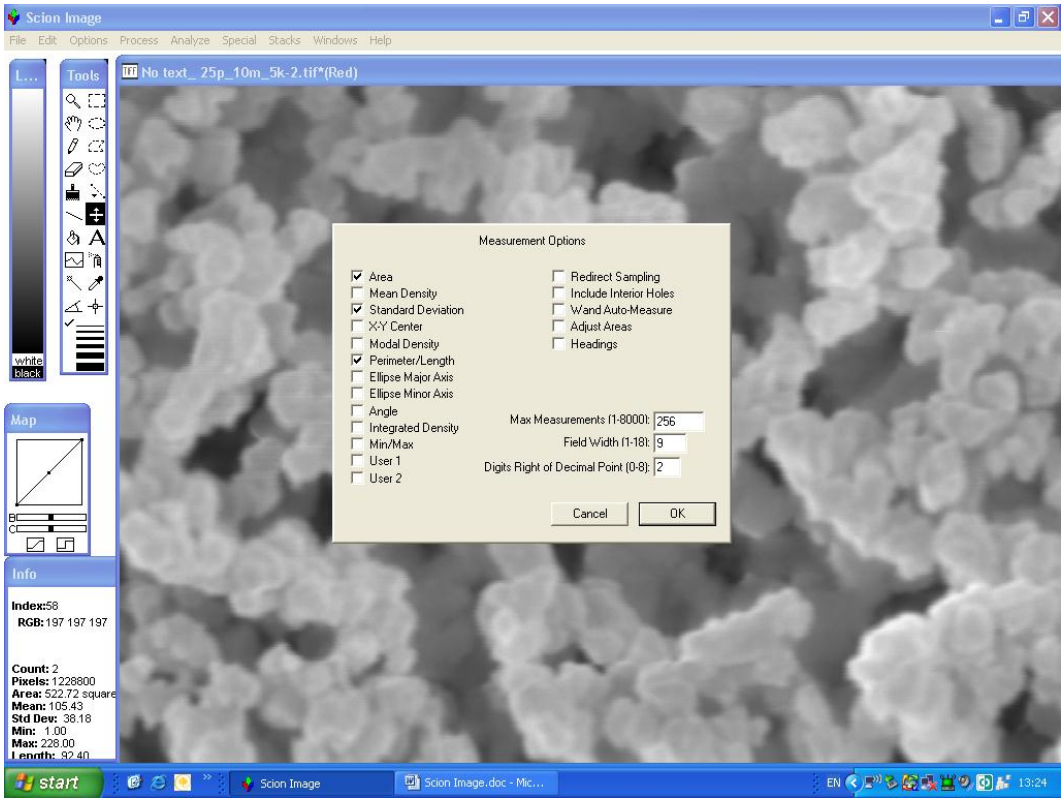

Figure B.7 The pop up window for setting area in the measurement options

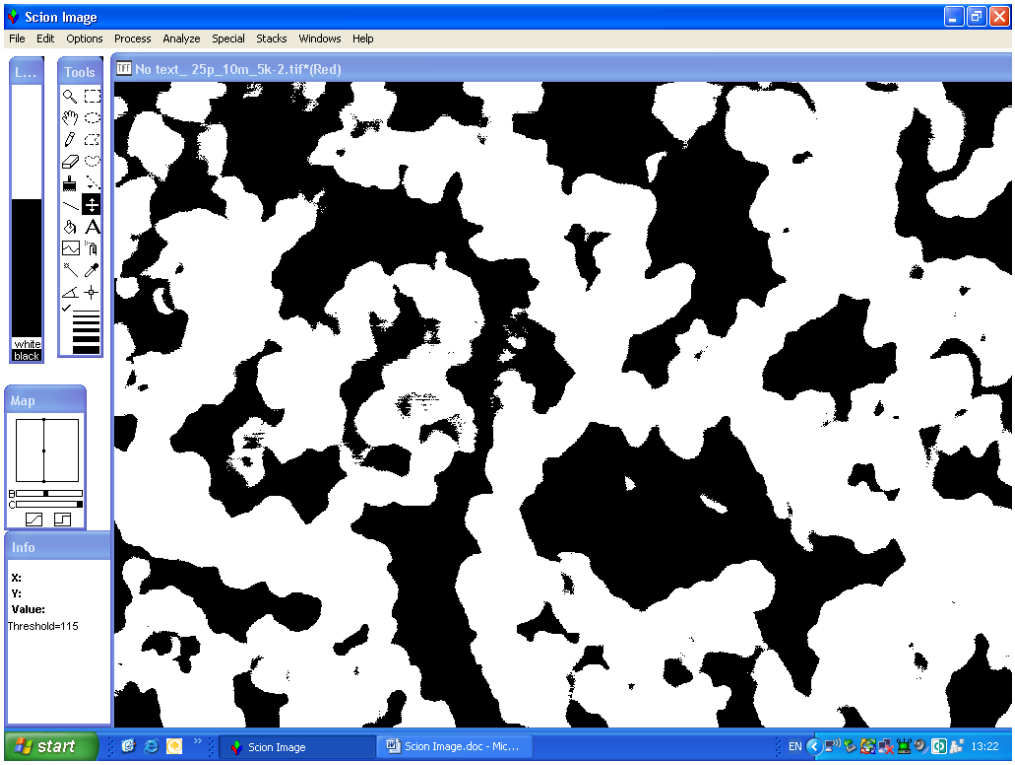

Figure B.8 Image when a threshold value is the default

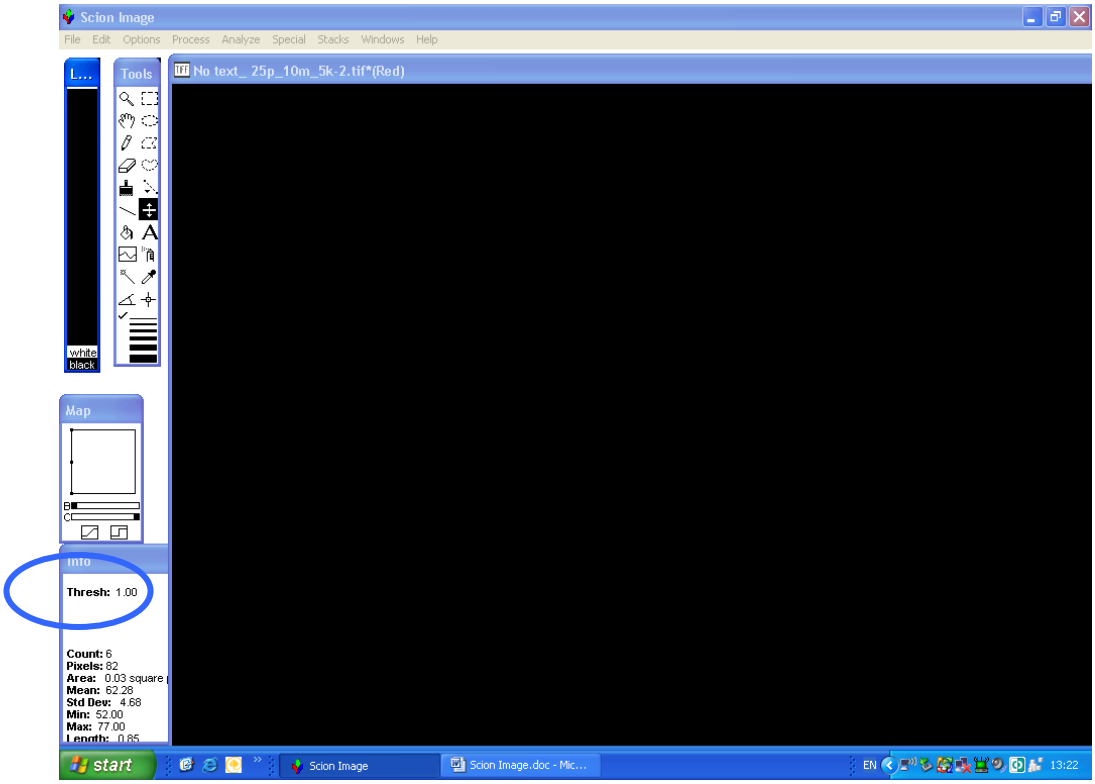

Figure B.9 Image when a threshold value is 1.0

Table B.1 Results of bead sizes of the monoliths prepared at different conditions estimated by Scion Image Analysis.

Times	Monoliths prepared by					
	25 wt % 10 min	**25 wt % 20 min**	**25 wt % 30 min**	**50 wt % 10 min**	**50 wt % 20 min**	**50 wt % 30 min**
1	1.85	1.89	1.78	0.26	0.22	0.14
2	1.52	1.90	2.19	0.26	0.26	0.16
3	1.85	1.97	1.74	0.37	0.26	0.15
4	1.48	1.86	1.86	0.25	0.24	0.15
5	1.73	1.76	1.91	0.35	0.21	0.23
6	2.13	1.79	1.71	0.29	0.25	0.16
7	1.98	2.0	2.23	0.31	0.29	0.20
8	1.83	1.98	2.10	0.35	0.17	0.15
9	1.90	1.75	2.37	0.30	0.20	0.17
10	1.54	1.83	1.98	0.24	0.23	0.19
11	1.68	1.84	2.01	0.27	0.22	0.16
12	1.67	1.73	2.03	0.32	0.25	0.16
13	1.70	1.77	1.68	0.28	0.25	0.17
14	1.63	1.72	1.75	0.27	0.20	0.22
15	1.72	1.72	1.49	0.24	0.20	0.21
16	1.78	1.98	1.92	0.26	0.22	0.21
17	1.76	1.87	1.87	0.29	0.26	0.18
18	1.53	1.76	1.70	0.28	0.24	0.18
19	1.73	1.54	2.00	0.24	0.24	0.20
20	1.80	1.64	1.84	0.26	0.21	0.22
21	1.57	1.67	1.82	0.22	0.22	0.21
22	1.59	1.83	1.92	0.21	0.20	0.17
23	1.85	1.60	1.68	0.31	0.24	0.16
24	1.82	1.78	1.51	0.22	0.20	0.14
25	1.86	1.69	1.32	0.28	0.22	0.18
26	1.8	1.74	1.90	0.31	0.19	0.15
27	1.68	1.78	1.36	0.22	0.17	0.22
28	1.62	2.01	1.48	0.21	0.22	0.22
29	1.74	1.99	1.48	0.25	0.22	0.16
30	1.70	1.85	1.87	0.26	0.26	0.19
31	1.88	1.78	1.67	0.27	0.21	0.15
32	1.88	1.62	1.87	0.24	023	0.20
33	1.69	1.77	2.08	0.33	0.20	0.18
34	2.00	1.75	1.85	0.19	0.28	0.21
35	2.05	1.75	1.65	0.23	0.22	0.21
36	1.68	1.82	1.53	0.26	0.23	0.20
37	1.97	1.85	1.65	0.21	0.20	0.16
38	1.98	1.86	1.62	0.26	0.22	0.19
39	1.52	1.65	1.87	0.30	0.20	0.22
40	1.65	1.70	1.84	0.37	0.18	0.15
Average Length (μm)	1.910 ± 0.210	1.876 ± 0.185	1.818 ± 0.162	0.250 ± 0.100	0.224 ± 0.036	0.193 ± 0.026

APPENDIX C

Experimental Results in Part of the Preconcentration

Table C.1 Results of the adsorption of cysteine in the monolith when varying concentration in the range of 0.05-1 millimolar

Flow rate (μl/min)		Abs.	Dilute ratio	Concentration (millimolar)		Amount of cysteine (μmol)			Adsorption Efficiency (%)
Inlet	Outlet	Outlet	Outlet	Inlet	Outlet	Inlet	Outlet	Absorb	
10	7.4419	0.1170	-	0.05	0.0408	0.045	0.0286	0.0164	36.52
10	7.4434	0.1152			0.0401		0.0281	0.0168	37.52
10	7.4619	0.2023	-	0.1	0.0705	0.09	0.0493	0.0406	45.14
10	7.4051	0.2065			0.0719		0.0503	0.0396	44.00
10	7.4534	0.3504	-	0.2	0.1221	0.18	0.0855	0.0944	52.49
10	7.4248	0.3489			0.1216		0.0851	0.0948	52.69
10	7.4966	0.4605	-	0.3	0.1605	0.27	0.1123	0.1576	58.37
10	7.4968	0.4695			0.1636		0.1145	0.1554	57.56
10	7.4679	0.9269	-	0.5	0.3231	0.45	0.2262	0.2237	49.72
10	7.4885	0.9067			0.3161		0.2212	0.2287	50.82
10	7.4480	0.6903	1:1	0.7	0.4813	0.63	0.3369	0.2930	46.51
10	7.4652	0.7017	1:1		0.4892		0.3424	0.2875	45.63
10	7.4552	1.0107	1:1	1	0.7095	0.90	0.4967	0.4032	44.81
10	7.3724	1.052	1:1		0.7340		0.5138	0.3861	42.90

Table C.2 Average results of the adsorption of cysteine in the monolith when varying concentration in the range of 0.05-1 millimolar

Flow rate (μl/min)		Abs.	Dilute ratio	Concentration (millimolar)		Amount of cysteine (μmol)			Adsorption efficiency (%)
Inlet	Outlet	Outlet	Outlet	Inlet	Outlet	Inlet	Outlet	Absorb	
10	7.4426	0.1161	-	0.05	0.0404	0.045	0.0283	0.016	37.02 ±1.0860
10	7.4335	0.2044	-	0.1	0.0712	0.09	0.0498	0.0401	44.57 ± 0.4332
10	7.4391	0.3496	-	0.2	0.1219	0.18	0.0853	0.0946	52.59 ± 0.2371
10	7.4967	0.465	-	0.3	0.1621	0.27	0.1134	0.1565	57.96 ± 0.9509
10	7.4782	0.9168	-	0.5	0.3196	0.45	0.2237	0.2262	50.27 ± 1.1557
10	7.4566	0.6960	1 : 1	0.7	0.4853	0.63	0.3397	0.2902	46.07 ± 0.0210
10	7.4138	1.0352	1 : 1	1	0.7218	0.9	0.5052	0.3947	43.85 ± 2.0201

APPENDIX D

TCEP solution

In this study, tris[2-carboxyethyl] phosphine (TCEP) was used as the reducing agent in order to breaking the disulfide bond between cysteine and thiol groups on the monolith surface. TCEP hydrochloride can be a viable alternative to DTT as a reducing agent in crystallization set ups. TCEP hydrochloride is soluble in water to 310 grams per liter. TCEP hydrochloride is Tris(2-carboxyethyl)phosphine hydrochloride (Mr 286.65). TCEP hydrochloride is an odorless (non-volatile) reducing agent that is more stable and effective than dithiothreitol (DTT) or 2-Mercaptoethanol. Unlike DTT, TCEP hydrochloride retains its reducing power at acid pH (pH 5) and at pH above 7.5. TCEP hydrochloride is unreactive towards other functional groups found in proteins. TCEP hydrochloride concentrations in the reservoir and drop are typically in molar equivalent or molar excess to the sample concentration. If the sample concentration is 1 mM, one might use a final TCEP hydrochloride concentration of 1 to 3 mM in the drop.

Cysteine in solution was detected using UV spectrophotometer (U-3000) to examine its concentration. In a spectrophotometer, the concentration of the sample is determined as an absorbance based on the adsorption of the light. The standard curve of cysteine in TCEP was performed to further verify the concentration of cysteine eluted by TCEP solution. The interesting cysteine concentration is in the range of 0.01-1 millimolar, If the concentration of cysteine in TCEP and water expressed in the further experiment exceeds these ranges, it is necessary to dilute the concentration to ensure it is measurable.

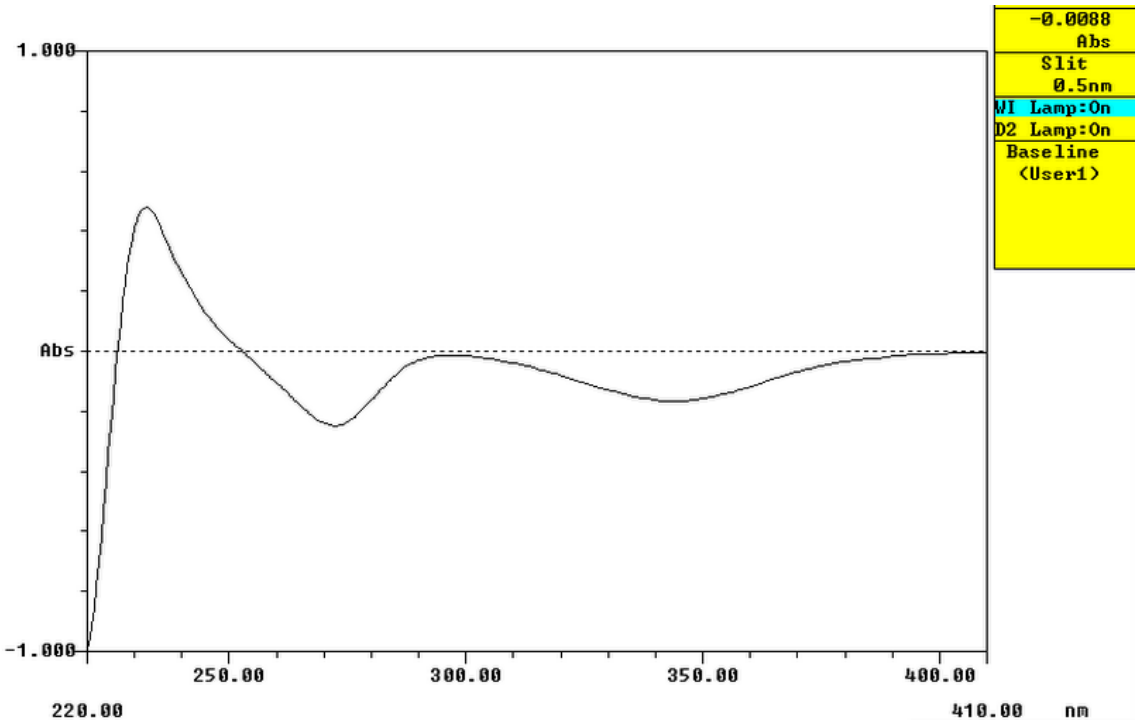

Figure D.1 Wavelength scan of 0.5-millimolar cysteine in TCEP solution**.**

Table D.1 Absorbance data of cysteine in TCEP measured at 232.5 nm

Concentration (millimolar)	Absorbance			Average
	#1	#2	#3	
0	0.0006	0.0005	0.0001	0.0004
0.1	0.0693	0.0723	0.0722	0.0713
0.3	0.1454	0.1398	0.1465	0.1439
0.5	0.2212	0.2241	0.2189	0.2214
0.7	0.3106	0.3115	0.3102	0.3108
1	0.4761	0.4783	0.4812	0.4785

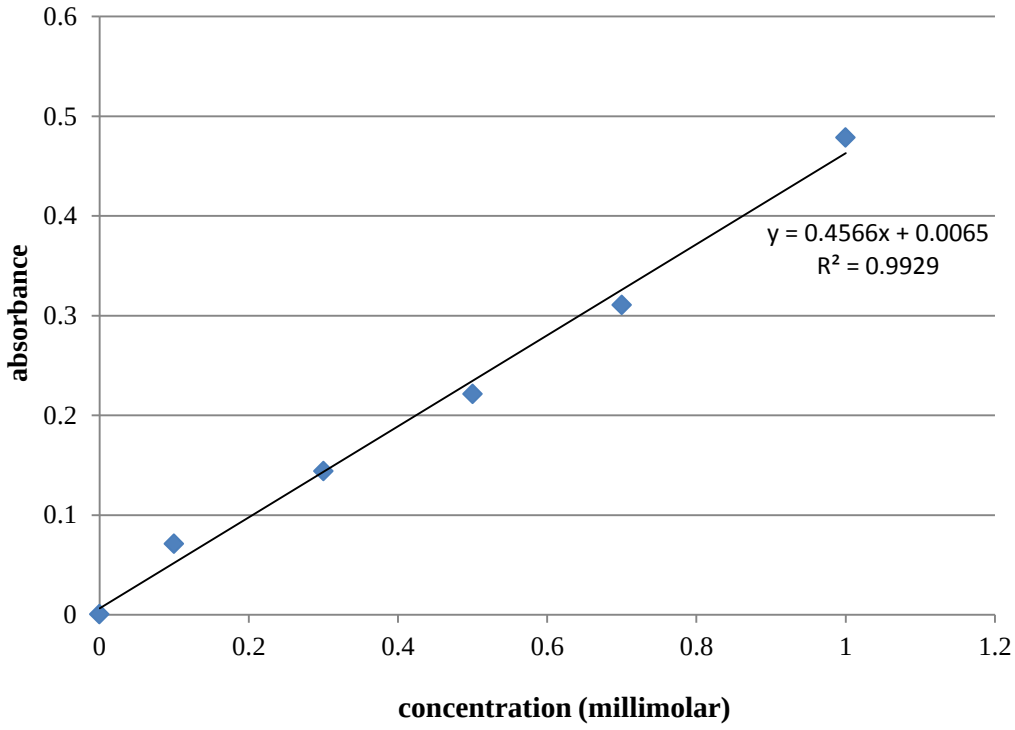

Figure D.2 Standard curve of cysteine in TCEP

APPENDIX E

Pressure drop calculation

Application of the porous monoliths in chromatography, solid-phase chemistry, or catalysis requires that a liquid be able to flow through the pores. As a result, resistance to flow is an important issue and the pressure needed to drive the liquid through the molded monolith should be as low as possible. Obviously, this can be achieved with materials that have a high content of large pores. However, as discussed earlier, the same applications may also require a large surface area and therefore a compromise has to be found for the seemingly contradictory requirements of low flow resistance and high surface area.

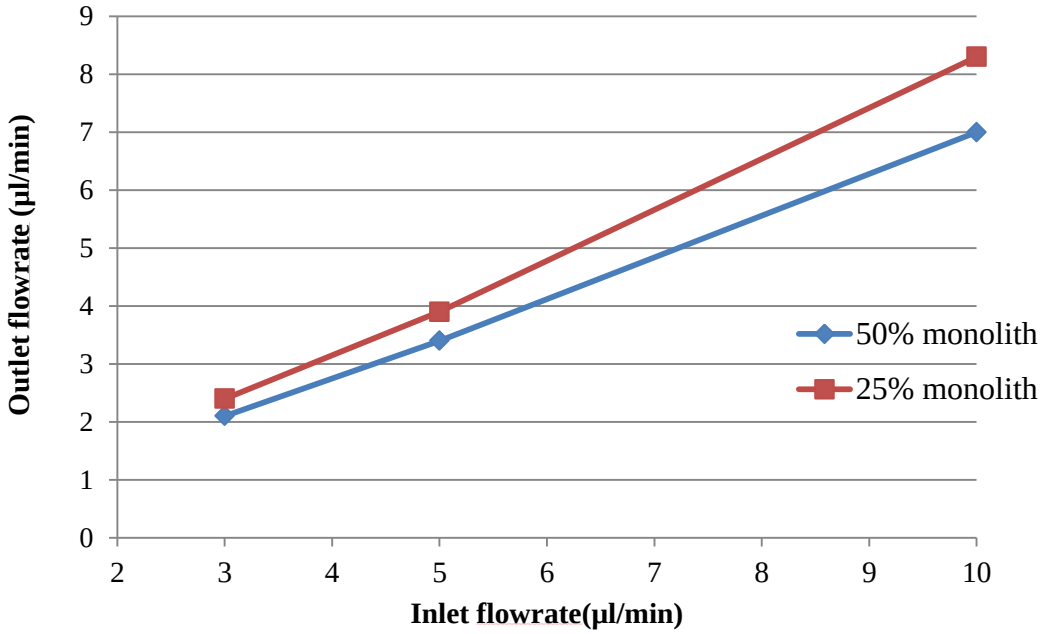

Figure E.1 Correlation between the flow inlet and the flow outlet of water through the monoliths prepared at various conditions.

As expected the outlet flow rates in every condition of the monoliths were less than the inlet flow rates as a result of the flow resistance to flow caused by the monolithic polymers. In addition, the outlet flow rates were linearly proportional to the inlet flow rates. The laminar flow resistance through porous monoliths can be examined using several equations, for example Darcy equation, Hagen Poiseulle equation (developed from Darcy equation for a circular tube), or Ergun equation. This study use development of Hagen Poiseulle equation. Theses equation gives the pressure drop in a fluid flowing through a packed bed in cylindrical pipe shown as following.

$$\Delta P = \left[\frac{17.3}{(Re)\,p} + 0.336\right]\frac{\rho_f u^2 L(1-\varepsilon)\varepsilon^{-4.8}}{d_p} \qquad \text{eq.1}$$

$$Re_p = \frac{d_p u \rho_f}{\mu} \qquad \text{eq.2}$$

Table E.1 Pressure drop calculation of monolith at various conditions.

Inlet flow (µl/min)	Pressure drop (MPa)	
	25% monolith for 30 min	50% monolith for 30 min
3	0.01	13.7
5	0.03	32.7
10	0.76	776.4

Table E.1 showed that although the higher flow rate was introduced, the outlet flow rate from the monolith prepared by 50 wt % 30 min was insignificantly different from those of other monoliths. Flow resistance allow liquid flow through the channel was not fully. The liquid might not penetrate through the pores inside the monolith. The adsorbate was not sufficiency to adsorb on the adsorbent surface then the adsorption efficiency was not too much. Howerver, a larger surface area would allow a larger amount of liquid solution to be transferred or to be adsorbed within the channel, resulting in a greater possibility of mass transfer. , the monolith with 50 wt% monomer polymerized for 30 min which had the highest surface area was chosen as an appropriate monolith for the preconcentration of cysteine solution.

CURRICULUM VITAE

NAME Miss Nisarat Promtrakulchai

DATE OF BIRTH 18 August 1986

EDUCATIONAL RECORD

HIGH SCHOOL	High School Graduation Satri Wat Absornsawan School, 2005
BACHELOR'S DEGREE	Bachelor of Engineering (Chemical Engineering) King Mongkut's University of Technology Thonburi, University, 2009
MASTER'S DEGREE	Master of Engineering (Chemical Engineering) King Mongkut's University of Technology Thonburi, 2011